

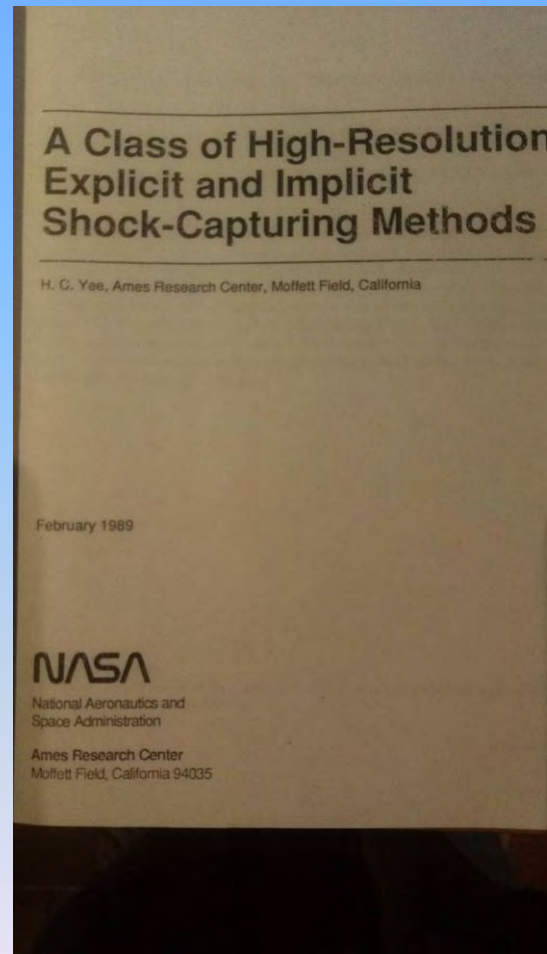


淡江大學航空太空工程學系

AUSMD Fluxes for Simulations of the Shock Waves and Droplets Problems

Yang-Yao Niu

Department of Aerospace Engineering, Tamkang University,
New Taipei City, Taiwan





- A+

for My CFD course of PhD study at Ohio-State University due to short course lecture notes of TVD, ENO reorganized by H. Yee and introduced by J. Y. Yang





Flux vector Splitting and Flux Difference

1. **Steger and Warming flux vector splitting scheme 1981 --- large dissipation**
2. **Van Leer Flux Splitting Scheme 1982--- large dissipation**
 - a. **AUSM(1993) AUSM+(1996) Meng Liou**
 - b. **AUSM+up(2006) by CH Chang and Meng Liou**
 - c. **AUSMD , AUSMV, AUSMDV (1994-1997)**
by Wada & Liou- \rightarrow mass flux allows more choices for contact discontinuities,
Niu(2001) for 7-eq. Two-fluid model.
3. **Roe Flux Differencing: The Approximate Riemann flux 1983, HLL, HLLC, HLLE.....**



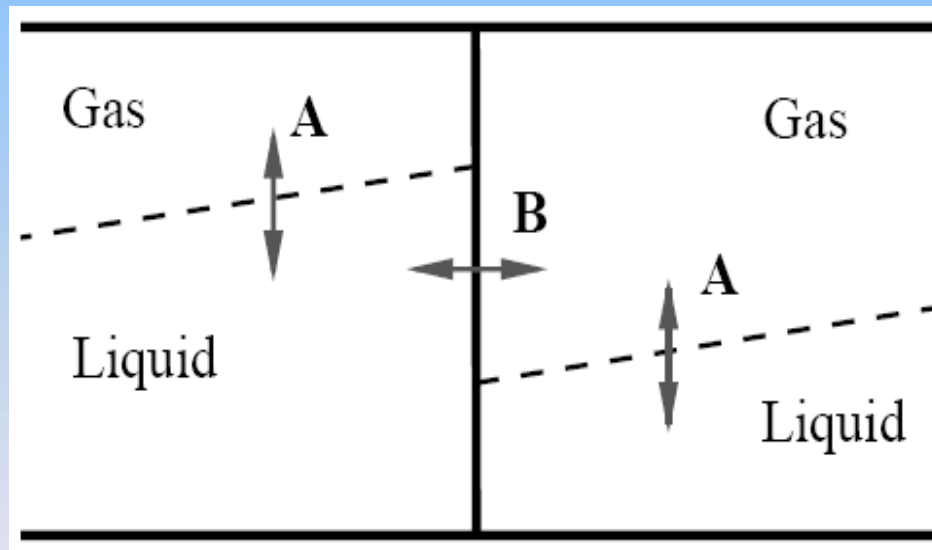
Successfully Flux Splitting for Two component flows

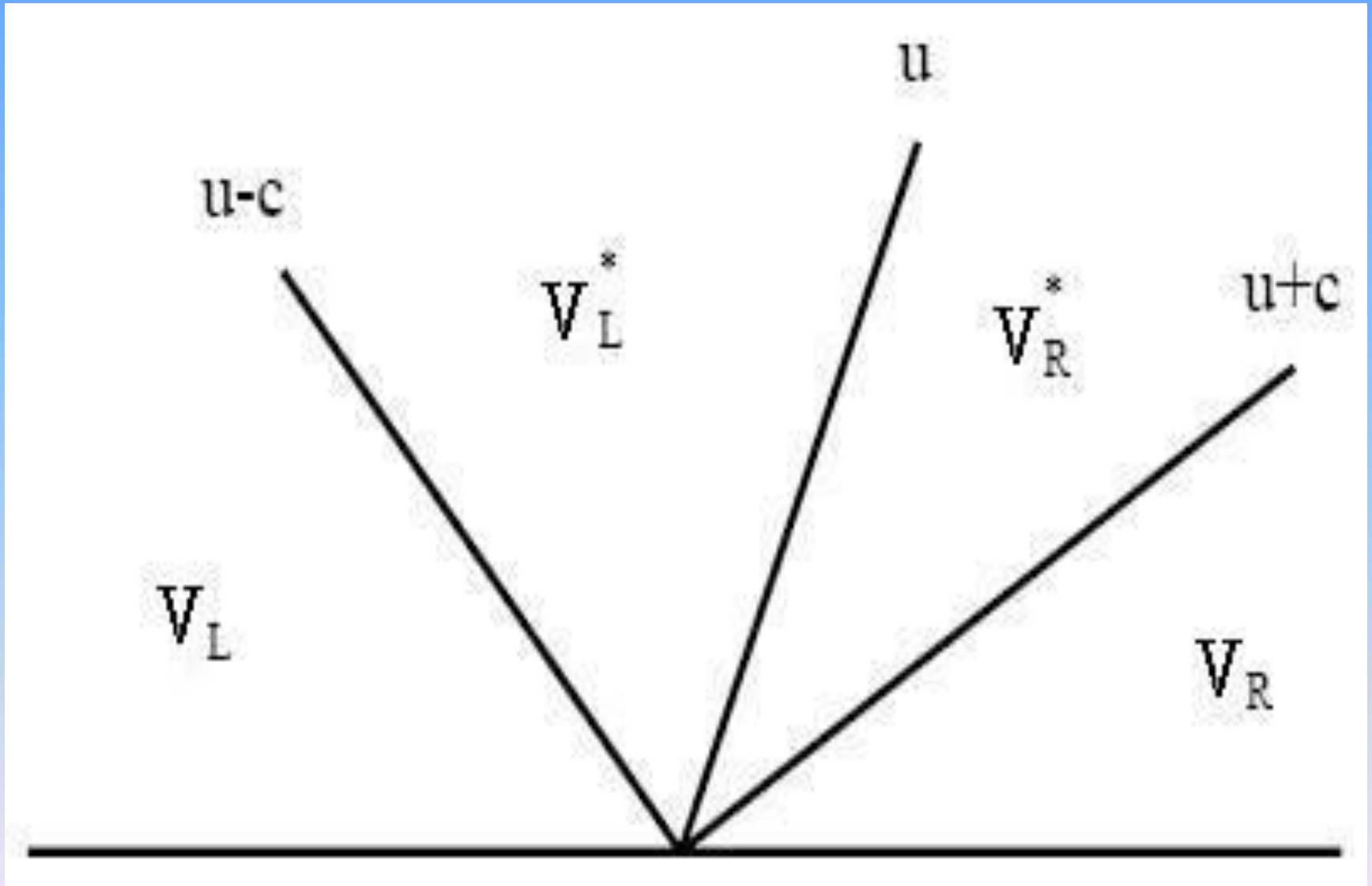
- A. AUSM+up works well for gas-gas flow and liquid-liquid flow, but failed at computing gas-liquid flows at interfaces so exact Riemann solver for liquid-gas interface is required
- B. AUSMD, its mass flux allows easy implementation of evaluating the variables on interfaces of gas-liquid
- C. Approximate Riemann fluxes as Roe HLLC, HLLE..... need figuring out tedious eigensystem



Numerical Flux

Exact or Approximated Riemann solvers are used to look for a robust scheme can be applied to the entire gas-gas, liquid-liquid and gas-liquid interface consistently







Characteristic equations

$$dp - \rho a du = 0 \quad \text{along} \quad dx/dt = u - a$$

$$dp - a^2 d\rho = 0 \quad \text{along} \quad dx/dt = u$$

$$dp + \rho a du = 0 \quad \text{along} \quad dx/dt = u + a$$

$$C = \rho a$$

$$\bar{p} + C_L \bar{u}_L = p_L + C_L u_L \quad \text{along the characteristic of speed } u + a$$

$$\bar{p} - C_R \bar{u}_R = p_R - C_R u_R \quad \text{along the characteristic of speed } u - a$$



The complete solution for numerical flux of the liquid-liquid interace and gas-gas interface

$$\bar{p} = \frac{1}{C_L + C_R} \left[C_R p_L + C_L p_R + C_L C_R (u_L - u_R) \right] ,$$

$$\bar{u} = \frac{1}{C_L + C_R} \left[C_L u_L + C_R u_R + (p_L - p_R) \right] ,$$

$$\bar{\rho}_L = \rho_L + (\bar{p} - p_L) / a_L^2 ,$$

$$\bar{\rho}_R = \rho_R + (\bar{p} - p_R) / a_R^2 ,$$

$$\bar{\rho} = \frac{1}{2} (\bar{\rho}_L + \bar{\rho}_R) , \quad \bar{a} = \frac{1}{2} (a_L + a_R)$$



gas-gas interface become

$$p_{g-g}^* = \frac{1}{2} \left[p_L + p_R + (u_L^g - u_R^g) / \bar{\rho} \bar{a} \right] ,$$

$$u_{g-g}^* = \frac{1}{2} \left[u_L^g + u_R^g + (p_L^g - p_R^g) / \bar{\rho} \bar{a} \right] ,$$

$$\rho_{L,g-g}^* = \rho_L^g + (p_{g-g}^* - p_L^g) / a_L^2 ,$$

$$\rho_{R,g-g}^* = \rho_R^g + (p_{g-g}^* - p_R^g) / a_R^2 ,$$

$$\rho_{g-g}^* = \frac{1}{2} \left(\rho_{L,g-g}^* + \rho_{R,g-g}^* \right) .$$



For the gas-gas interface,
AUSMD flux

$$E_{g-g} = \frac{1}{2} \left[\left(\rho_{g-g}^* u_{g-g}^* \right)_{1/2} (\Psi_L + \Psi_R) - \left| \left(\rho_{g-g}^* u_{g-g}^* \right) \right| (\Psi_R - \Psi_L) \right] + P_{1/2},$$

where

$$\Psi_L = \begin{pmatrix} 1 \\ u_L \\ H_L \\ Y_L \end{pmatrix}, \quad \Psi_R = \begin{pmatrix} 1 \\ u_R \\ H_R \\ Y_R \end{pmatrix} \quad \text{and} \quad P = \begin{pmatrix} 0 \\ p_{g-g}^* \\ 0 \\ 0 \end{pmatrix}.$$



liquid-liquid interface become

$$p_{l-l}^* = \frac{1}{2} \left[p_L^l + p_R^l + (u_L^l - u_R^l) / \bar{\rho} \bar{a} \right] ,$$

$$u_{l-l}^* = \frac{1}{2} \left[u_L^l + u_R^l + (p_L^l - p_R^l) / \bar{\rho} \bar{a} \right] ,$$

$$\rho_{L,l-l}^* = \rho_L^l + (p_{l-l}^* - p_L^l) / a_L^2 ,$$

$$\rho_{R,l-l}^* = \rho_R^l + (p_{l-l}^* - p_R^l) / a_R^2 ,$$

$$\rho_{l-l}^* = \frac{1}{2} \left(\rho_{L,l-l}^* + \rho_{R,l-l}^* \right) .$$



For the liquid-liquid interface

$$E_{l-l} = \frac{1}{2} \left[\left(\rho_{l-l}^* u_{l-l}^* \right)_{1/2} (\Psi_L + \Psi_R) - \left| \left(\rho_{l-l}^* u_{l-l}^* \right) \right| (\Psi_R - \Psi_L) \right] + P_{1/2},$$

Where

$$\Psi_L = \begin{pmatrix} 1 \\ u_L \\ H_L \\ Y_L \end{pmatrix}, \quad \Psi_R = \begin{pmatrix} 1 \\ u_R \\ H_R \\ Y_R \end{pmatrix} \quad \text{and} \quad P_{1/2} = \begin{pmatrix} 0 \\ p_{l-l}^* \\ 0 \\ 0 \end{pmatrix}.$$



By choosing

$$C_L = \rho_L^g a_L^g \quad \text{and} \quad C_R = \rho_R^l a_R^l.$$

The complete solutions of gas-liquid interface can be

$$p_{g-l}^* = \frac{1}{C_L + C_R} \left[C_R p_L^g + C_L p_R^l + C_L C_R (u_L^g - u_R^l) \right],$$

$$u_{g-l}^* = \frac{1}{C_L + C_R} \left[C_L u_L^g + C_R u_R^l + (p_L^g - p_R^l) \right], \quad (51)$$

$$\rho_{L,g-l}^* = \rho_L^g + (p_{g-l}^* - p_L^g) / a_L^2,$$

$$\rho_{R,g-l}^* = \rho_R^g + (p_{g-l}^* - p_R^l) / a_R^2,$$

$$\rho_{g-l}^* = \frac{1}{2} (\rho_{L,g-l}^* + \rho_{R,g-l}^*),$$



For the gas-liquid interface

$$E_{g-l} = \frac{1}{2} \left[\left(\rho_{g-l}^* u_{g-l}^* \right)_{1/2} (\Psi_L + \Psi_R) - \left| \left(\rho_{g-l}^* u_{g-l}^* \right) \right| (\Psi_R - \Psi_L) \right] + P_{1/2},$$

Where

$$\Psi_L = \begin{pmatrix} 1 \\ u_L \\ H_L \\ Y_L \end{pmatrix}, \quad \Psi_R = \begin{pmatrix} 1 \\ u_R \\ H_R \\ Y_R \end{pmatrix} \quad \text{and} \quad P_{1/2} = \begin{pmatrix} 0 \\ p_{g-l}^* \\ 0 \\ 0 \end{pmatrix}.$$



By choosing

$$C_L = \rho_L^l a_L^l \quad \text{and} \quad C_R = \rho_R^g a_R^g$$

The complete solutions of liquid-gas interface can be

$$p_{l-g}^* = \frac{1}{C_L + C_R} \left[C_R p_L^l + C_L p_R^g + C_L C_R (u_L^l - u_R^g) \right] ,$$

$$u_{l-g}^* = \frac{1}{C_L + C_R} \left[C_L u_L^l + C_R u_R^g + (p_L^l - p_R^g) \right] , \quad (52)$$

$$\rho_{L,l-g}^* = \rho_L^l + (p_{l-g}^* - p_L) / a_L^2 ,$$

$$\rho_{R,l-g}^* = \rho_R^g + (p_{l-g}^* - p_R) / a_R^2 ,$$

$$\rho_{l-g}^* = \frac{1}{2} (\rho_{L,l-g}^* + \rho_{R,l-g}^*)$$



For the liquid-gas interface

$$E_{l-g} = \frac{1}{2} \left[\left(\rho_{l-g}^* u_{l-g}^* \right)_{1/2} (\Psi_L + \Psi_R) - \left| \left(\rho_{l-g}^* u_{l-g}^* \right) \right| (\Psi_R - \Psi_L) \right] + P_{1/2},$$

Where

$$\Psi_L = \begin{pmatrix} 1 \\ u_L \\ H_L \\ Y_L \end{pmatrix}, \quad \Psi_R = \begin{pmatrix} 1 \\ u_R \\ H_R \\ Y_R \end{pmatrix} \quad \text{and} \quad P_{1/2} = \begin{pmatrix} 0 \\ p_{l-g}^* \\ 0 \\ 0 \end{pmatrix}.$$



The general discretization form for each cell Ω_j
can be organized as

$$\Omega_j \partial_t \begin{pmatrix} \alpha_k \rho_k \\ \alpha_k \rho_k u_k \\ \alpha_k \rho_k E_k \end{pmatrix}_j + \sum \left(\overline{ab} E_{g-g} + \overline{bc} E_{l-g} + \overline{bc} E_{g-l} + \overline{cd} E_{l-l} \right)_m n_m S_m$$
$$+ \Omega_j \begin{pmatrix} 0 \\ 0 \\ p^{\text{int}} \partial_t \alpha_k \end{pmatrix}_j - \sum \begin{pmatrix} 0 \\ p^{\text{int}} \alpha_k \\ 0 \end{pmatrix}_m n_m S_m = \Omega_j \begin{pmatrix} 0 \\ \rho_k \alpha_k g \\ \rho_k \alpha_k u_k g \end{pmatrix}_j .$$



Here the subscript $k = g$ or l representing gas phase or liquid phase. The functions \overline{ab} , \overline{bc} and \overline{cd} are the effective length of each type of interfaces. We define

$$\overline{ab} = \min(\alpha_g^L, \alpha_g^R),$$

$$\overline{bc} = \max(0, \alpha_l^R - \alpha_g^L) \quad \text{or}$$

$$\overline{bc} = \max(0, \alpha_g^R - \alpha_l^L),$$

$$\overline{cd} = \min(\alpha_l^L, \alpha_l^R).$$



Current Works

1. Using the 4th order Runge - Kutta method with spatial difference uses 3rd order MUSCL extrapolation to solve a six-equation two fluid model.
2. Deriving AUSMD approximated Riemann flux of two-component flow.
 - Journal of Computational Physics, March, 2016
 - the 3D case has been published in Computers and Fluids. August, 2016



Two-Fluid Model

We use two kinds of conservative governing equation to solve numerical simulation in each phase then establish three conservative equations consist of mass, momentum and energy.

$$\frac{\partial Q}{\partial t} + \frac{\partial F}{\partial x} = H$$

$$Q = \begin{bmatrix} \alpha_g \rho_g \\ \alpha_l \rho_l \\ \alpha_g \rho_g u_g \\ \alpha_l \rho_l u_l \\ \alpha_g \rho_g E_g \\ \alpha_l \rho_l E_l \end{bmatrix} \quad F = \begin{bmatrix} \alpha_g \rho_g u_g \\ \alpha_l \rho_l u_l \\ \alpha_g \rho_g u_g^2 + \alpha_g p \\ \alpha_l \rho_l u_l^2 + \alpha_l p \\ \alpha_g \rho_g u_g H_g \\ \alpha_l \rho_l u_l H_l \end{bmatrix} \quad H = \begin{bmatrix} 0 \\ 0 \\ g_x \alpha_g \rho_g + p_{\text{int}} \nabla \alpha_g \\ g_x \alpha_l \rho_l + p_{\text{int}} \nabla \alpha_l \\ -p \frac{\partial \alpha_g}{\partial t} + g_x \alpha_g \rho_g u_g \\ -p \frac{\partial \alpha_l}{\partial t} + g_x \alpha_l \rho_l u_l \end{bmatrix}$$



Two-Fluid model

The common two-fluid model (RELAP5-3D ,CATHARE codes) is widely used in Thermal Hydraulic codes

--but brings numerical difficulties. One of the issues is its non-hyperbolicity, making the system an ill-posed problem, presented as numerical instability.

The ways to cure the non-hyperbolicity, always requires additional terms or assumptions,

- the interfacial pressure force (Stuhmiller, 1997)
- virtual mass force (Bestion, 1990)
- two-pressure model or volume fraction transport equation (Baer and Nunziato (1986), Saurel, Abgrall (1999), (Niu, 2001),.....), five equation model.....



Interfacial pressure term

$$p_{\text{int}} = p - \sigma \frac{\alpha_g \rho_g \alpha_l \rho_l}{\alpha_g \rho_l + \alpha_l \rho_g} (u_g - u_l)^2$$

Where σ is a parameter and the system becomes weakly hyperbolic if

$$\sigma \geq 1$$



Equation of state

Liquid Phase EOS :

$$P_l = \frac{\gamma_l - 1}{\gamma_l} \rho_l C_{pl} T_l - p_\infty \quad \text{Stiffened Gas E.O.S.}$$

$$\rho_l = 998.23 \frac{\text{kg}}{\text{m}^3} \quad \gamma_l = 1.932 \quad C_{pl} = 8095.08 \frac{\text{J}}{\text{kg} \cdot \text{K}} \quad p_\infty = 1.1645 \times 10^9 \text{ Pa}$$

Gas Phase EOS :

$$P_g = \rho_g R_g T_g \quad \text{Ideal Gas E.O.S.}$$

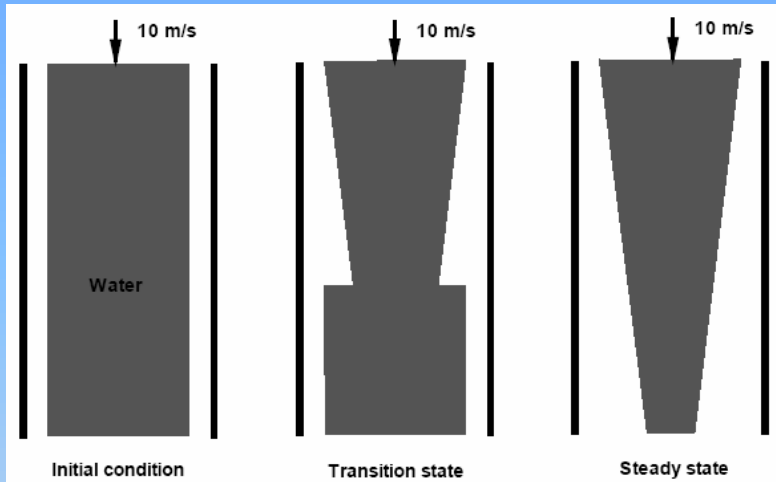
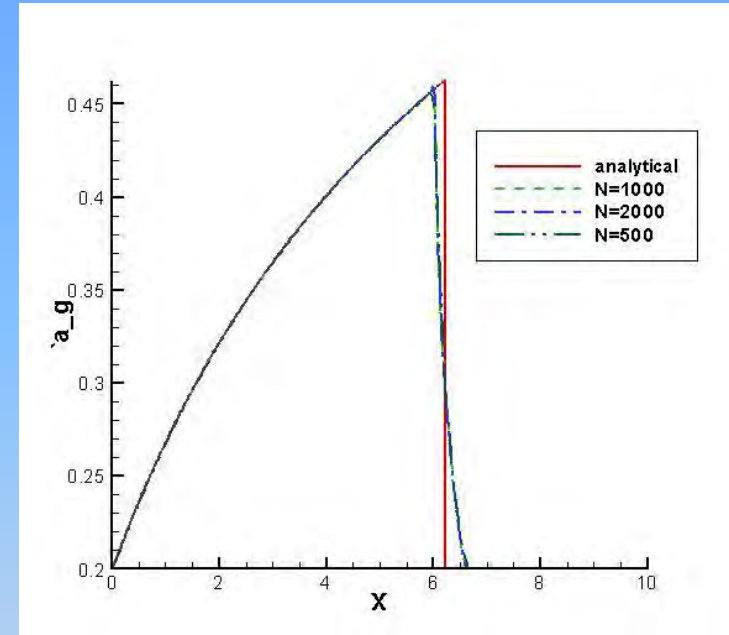


Illustration of Ransom's water faucet problem.



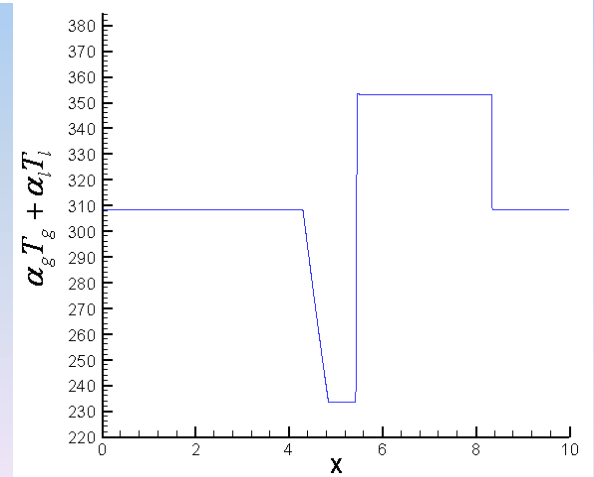
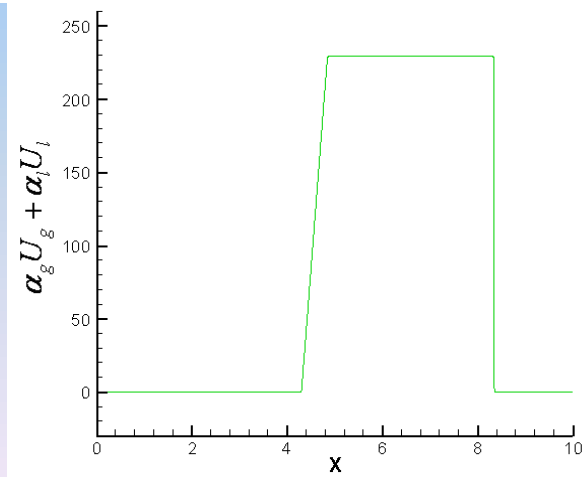
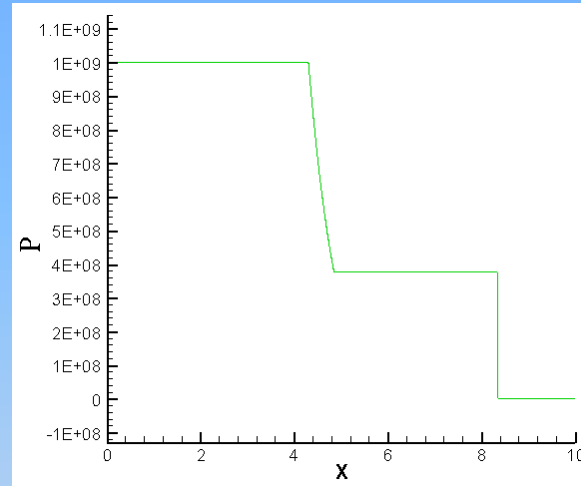
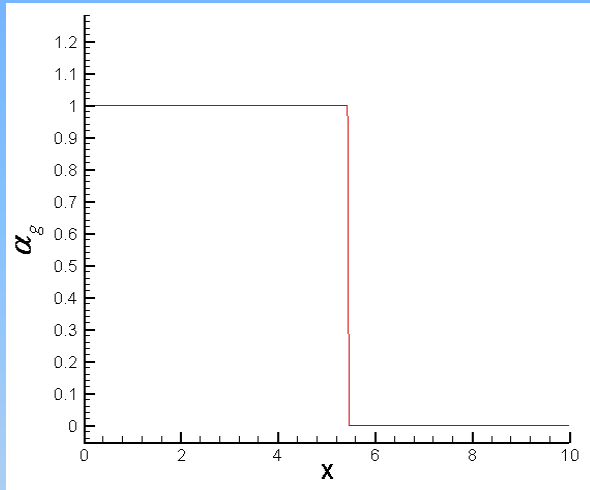
Several different grids are used in the water faucet problem.



淡江大學航空太空工程學系

$$(p, \alpha_g, u_i, T_i)_L = (1.0 \times 10^9 \text{ pa}, 1 - \varepsilon, 0 \text{ m/s}, 308.15 \text{ K}^0)$$

$$(p, \alpha_g, u_i, T_i)_R = (1.0 \times 10^5 \text{ pa}, \varepsilon, 0 \text{ m/s}, 308.15 \text{ K}^0)$$

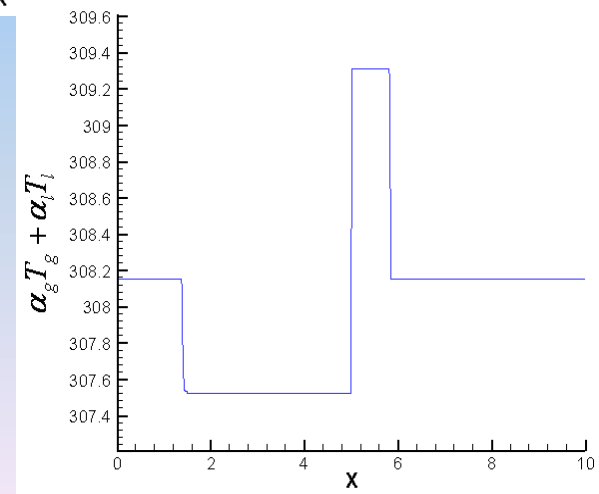
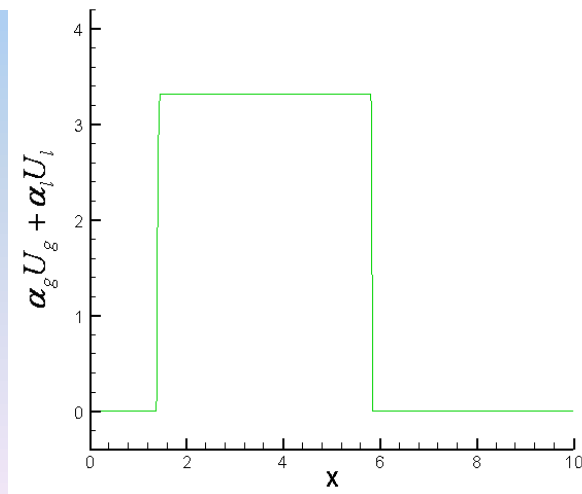
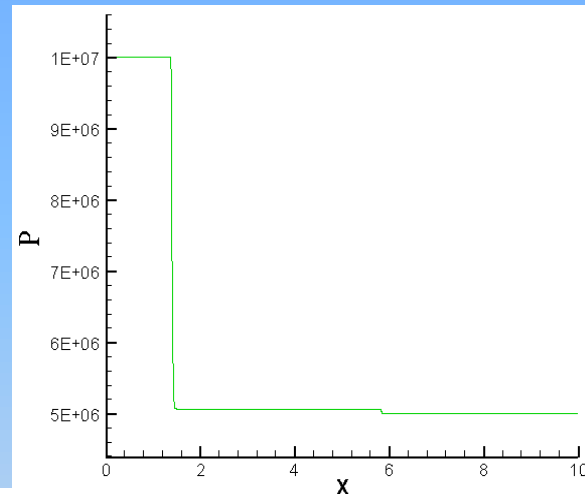
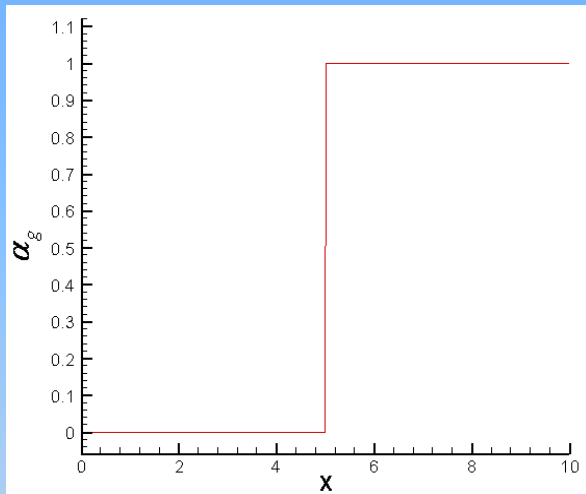




淡江大學航空太空工程學系

$$(p, \alpha_g, u_i, T_i)_L = (1.0 \times 10^7 \text{ pa}, \varepsilon, 0 \text{ m/s}, 308.15 \text{ K}^0)$$

$$(p, \alpha_g, u_i, T_i)_R = (5.0 \times 10^6 \text{ pa}, 1 - \varepsilon, 0 \text{ m/s}, 308.15 \text{ K}^0)$$





Left: $P = 4.18375 \times 10^6 \text{ Pa}$

$$u_i = 1.818957 \times 10^3 \text{ m/s}$$

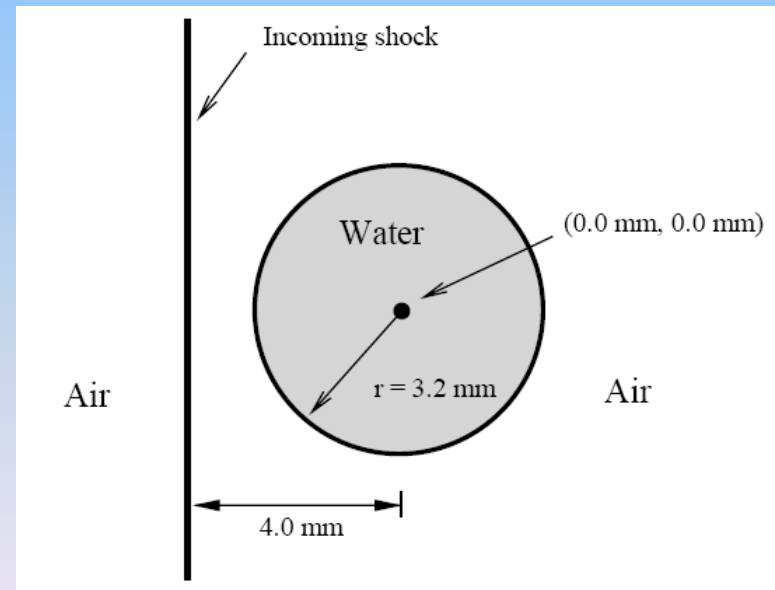
$$v_i = 0 \text{ m/s}$$

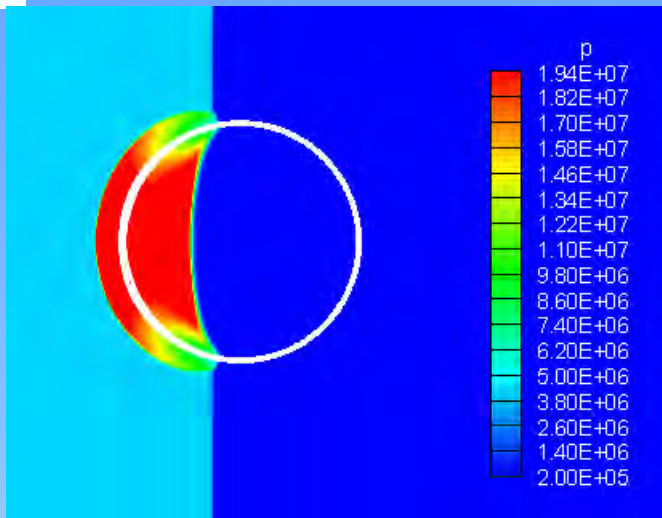
$$T_i = 2755.48 \text{ K}$$

Right: $P = 1.0 \times 10^5 \text{ Pa}$

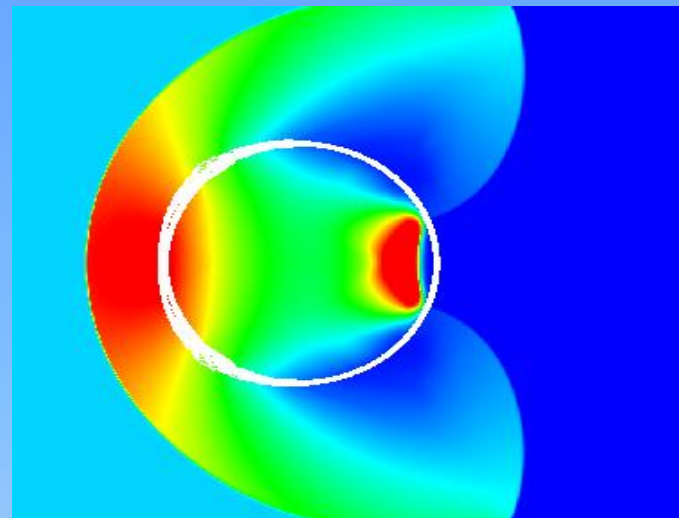
$$u_i = v_i = 0 \text{ m/s}$$

$$T_i = 346.98 \text{ K}$$

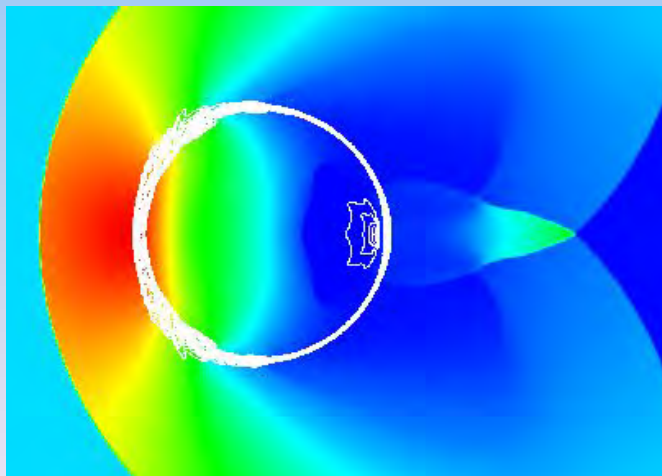




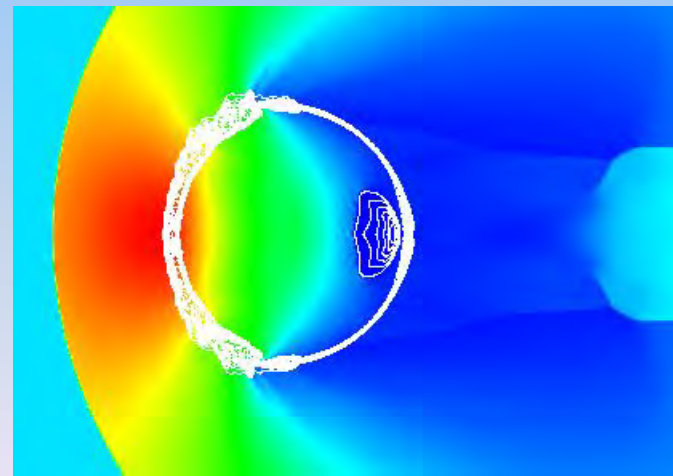
(1) $t = 1.5 \mu s$



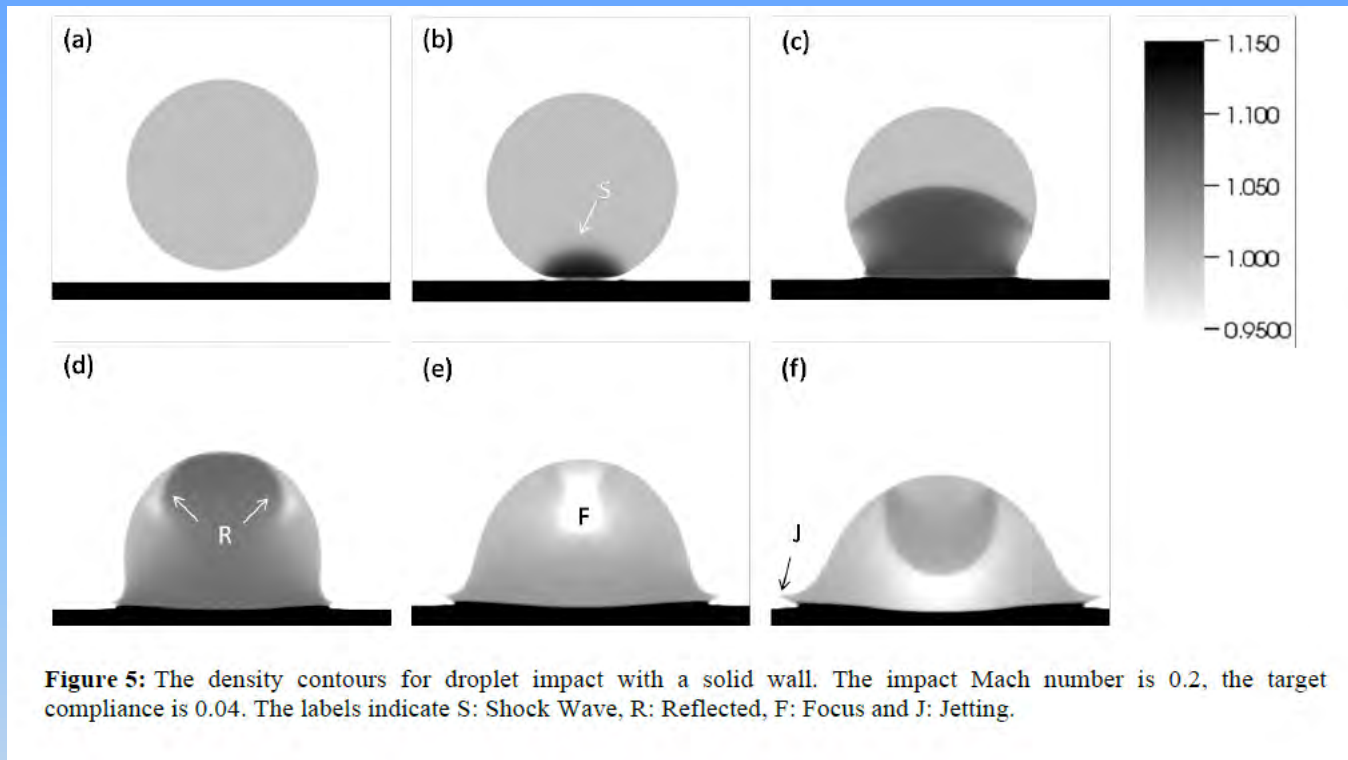
(2) $t = 4.0 \mu s$



(3) $t = 6.5 \mu s$



(4) $t = 9.0 \mu s$



Numerical Analysis of High Speed Droplet Impact

Toshiyuki Sanada^{*}, Keita Ando[†] and Tim Colonius[†]

^{*} Department of Mechanical Engineering, Shizuoka University, Hamamatsu, 432-8561, Japan

[†] Department of Mechanical Engineering, California Institute of Technology, Pasadena, CA 91106, USA

ttsanad@ipc.shizuoka.ac.jp, kando@caltech.edu and colonius@caltech.edu



2D high-speed water droplet impact dry wall

Initial Conditions :

Outside Droplet:

$$p = 1. \times 10^5 \text{ Pa}$$

$$u_i = v_i = 0 \text{ m/s}$$

$$T_i = 300 \text{ K}$$

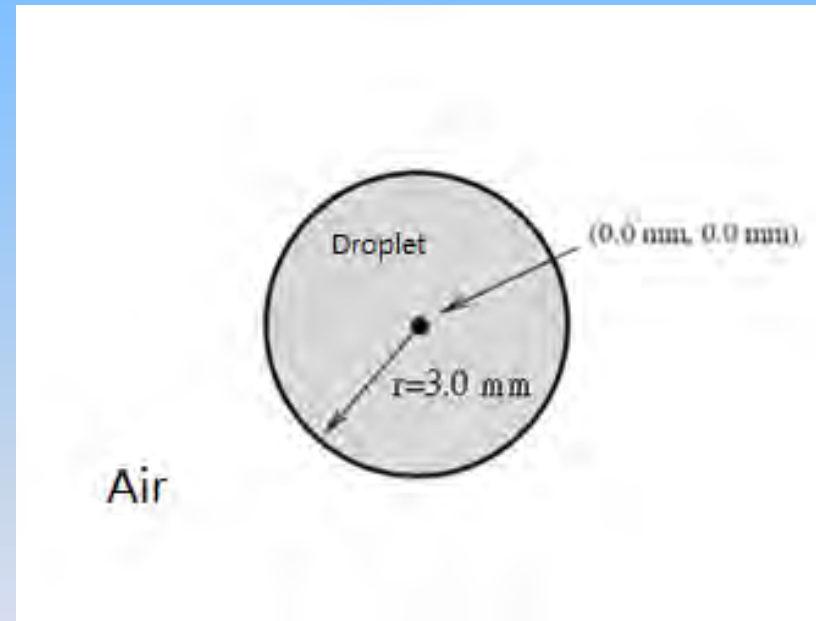
Inside Droplet:

$$p = 1.1 \times 10^5 \text{ Pa}$$

$$u_i = 200\text{-}500 \text{ m/s}$$

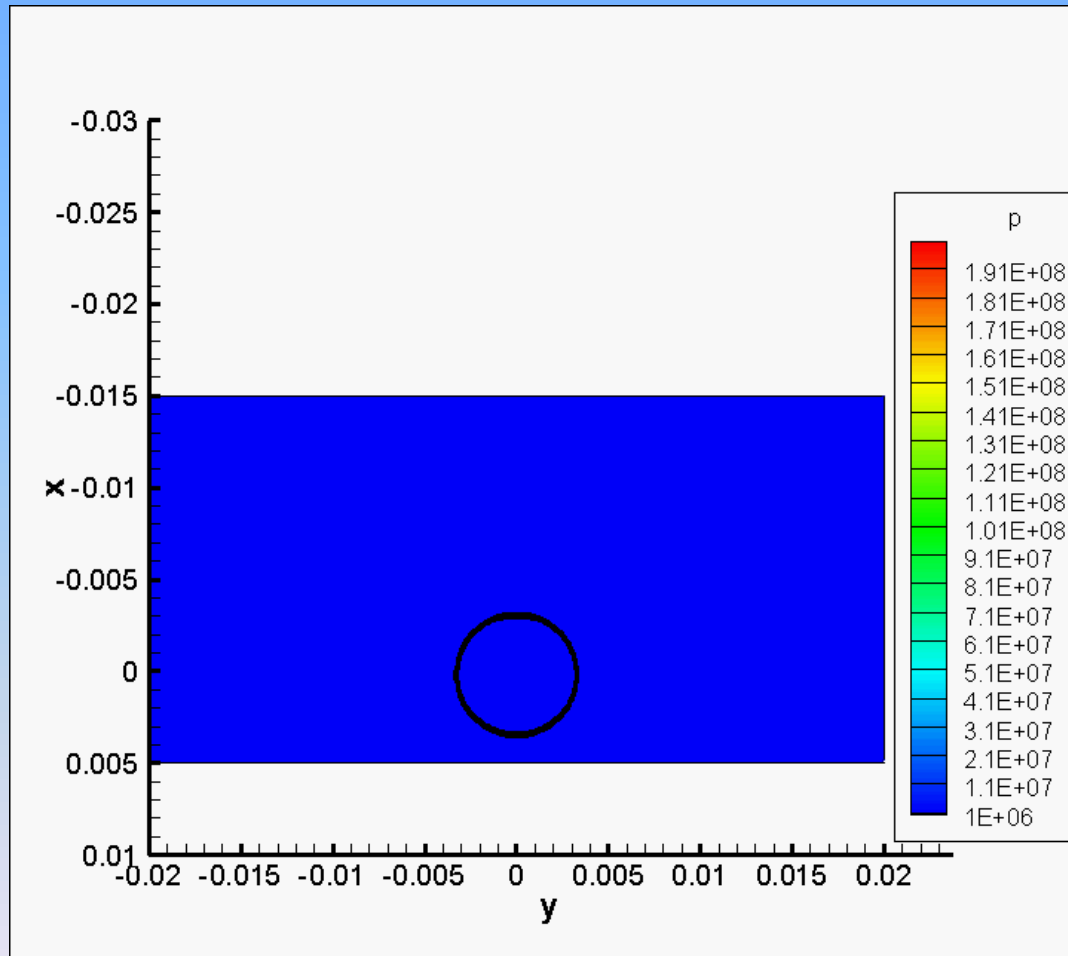
$$v_i = 0 \text{ m/s}$$

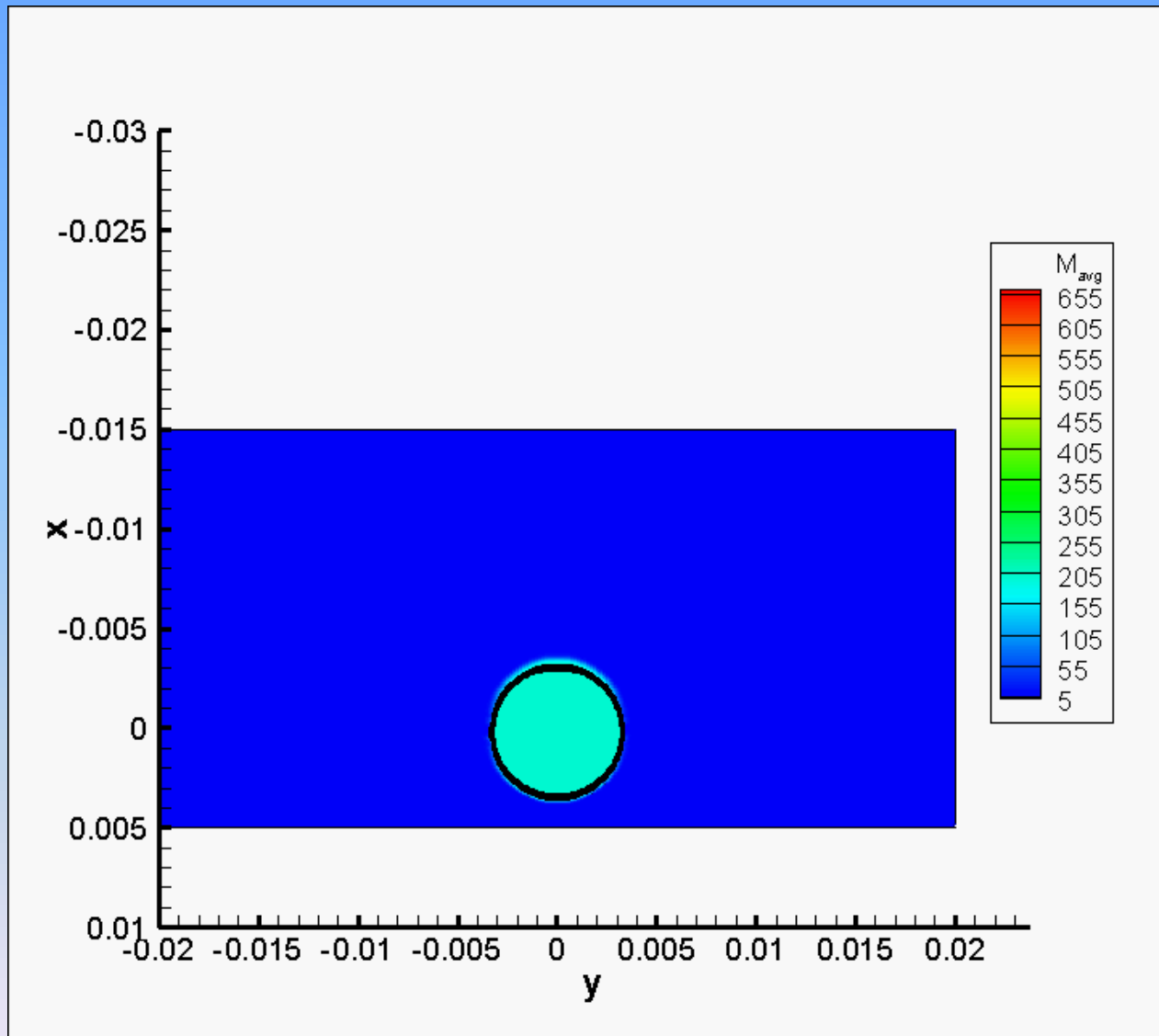
$$T_i = 300 \text{ K}$$





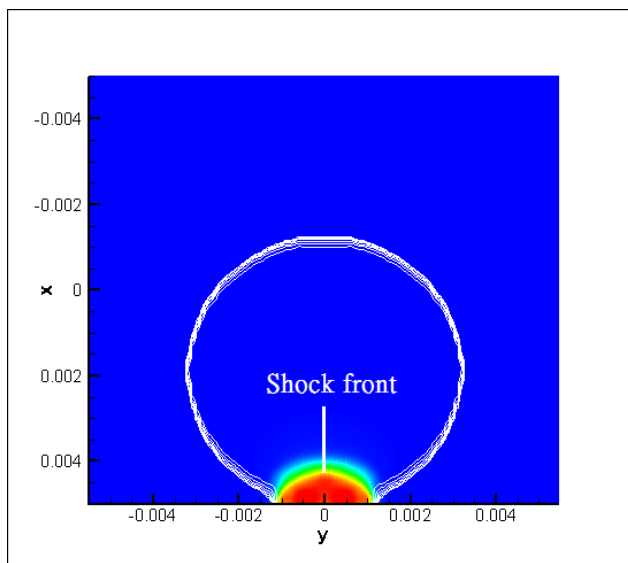
2D high-speed water droplet impact dry wall



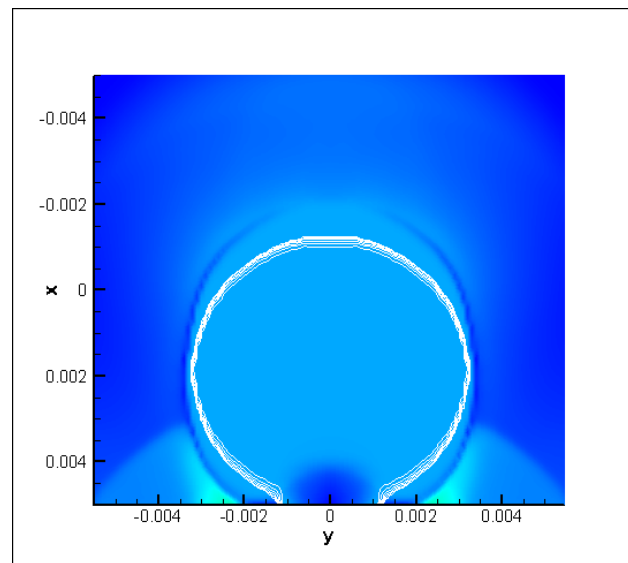




$t = 9.48\mu\text{s}$



Pressure

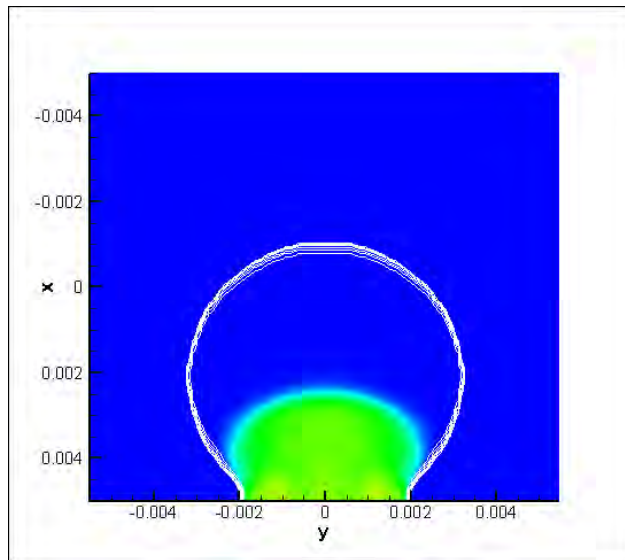


Velocity

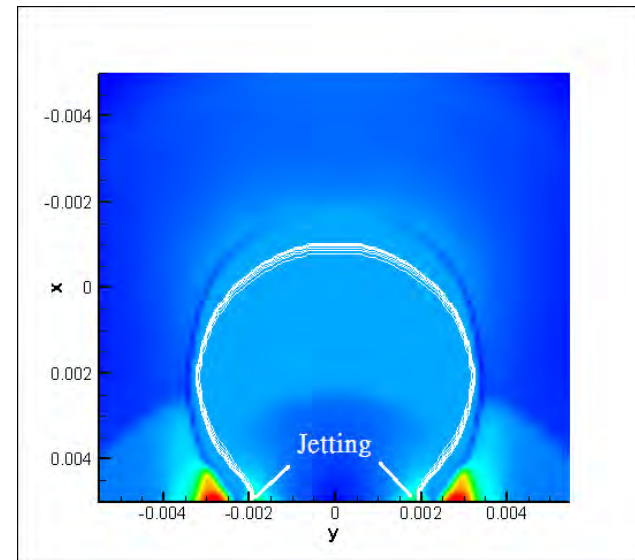
VOF



$t = 10.6\mu\text{s}$



Pressure

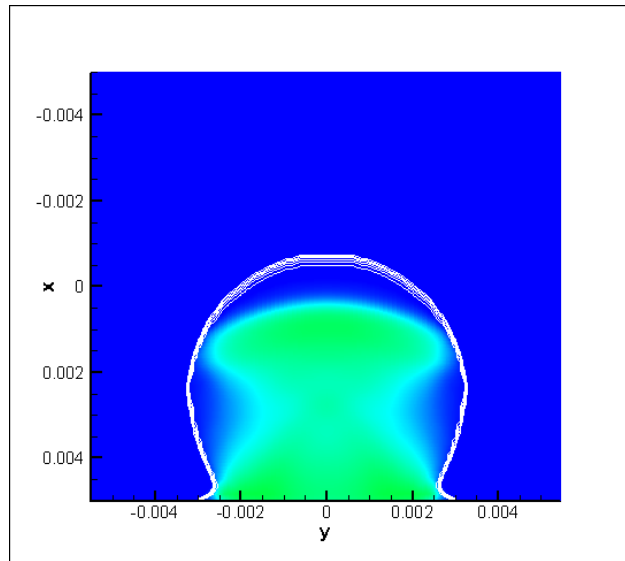


Velocity

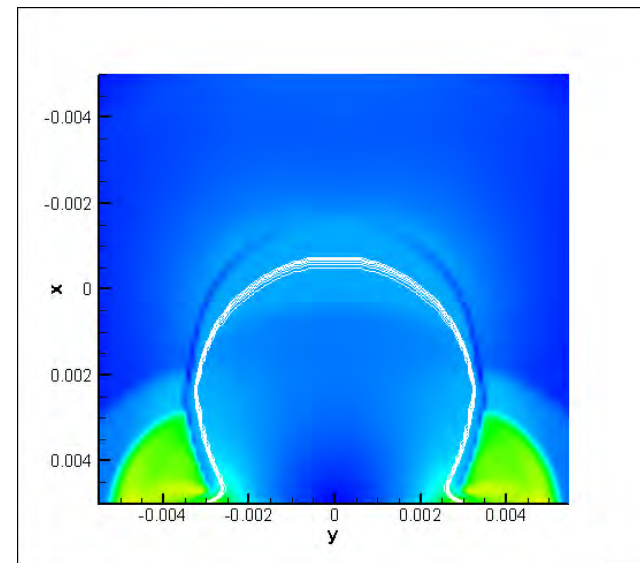
VOF



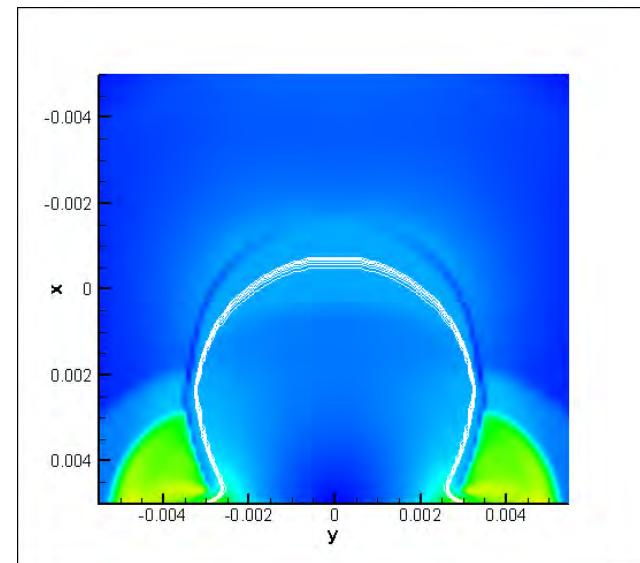
$t = 12.0\mu s$



Pressure



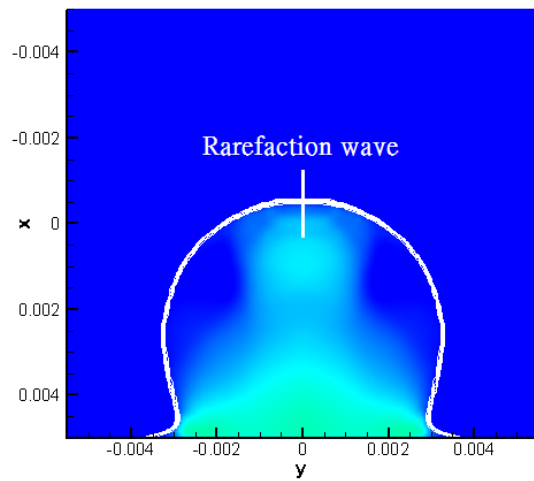
Velocity



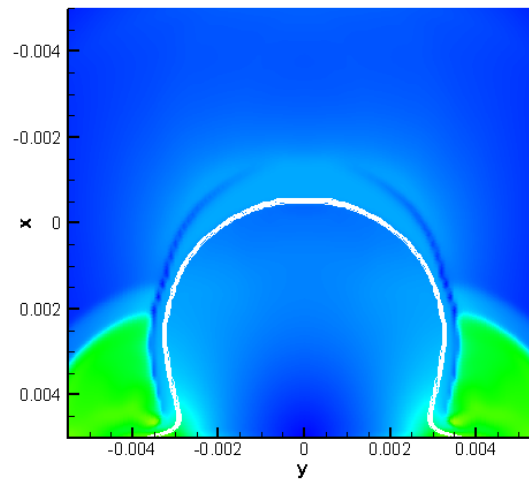
VOF



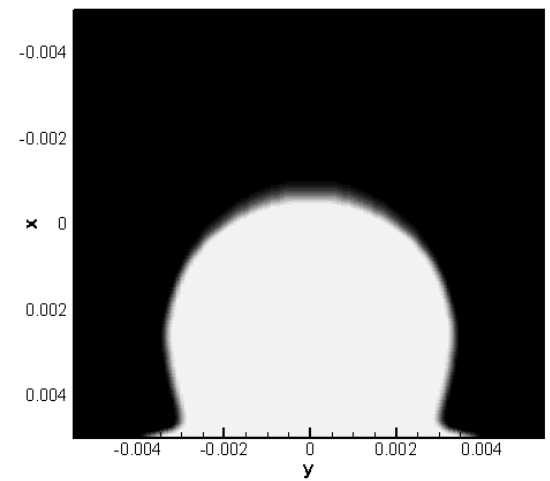
$t = 12.6\mu\text{s}$



Pressure



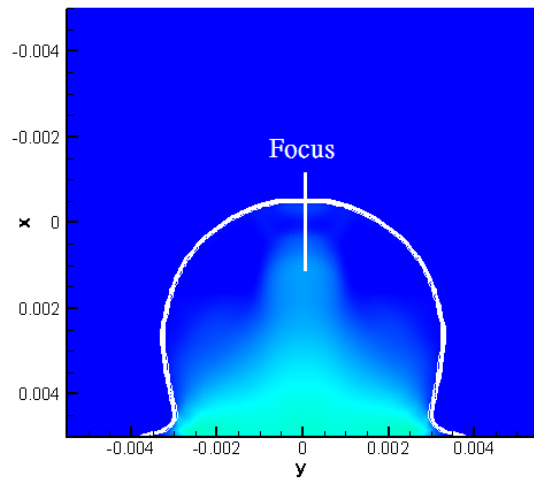
Velocity



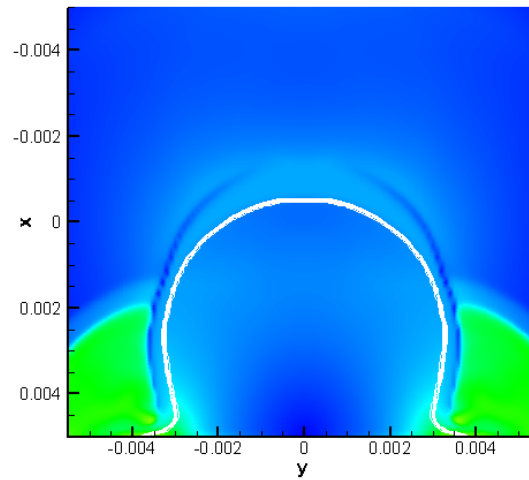
VOF



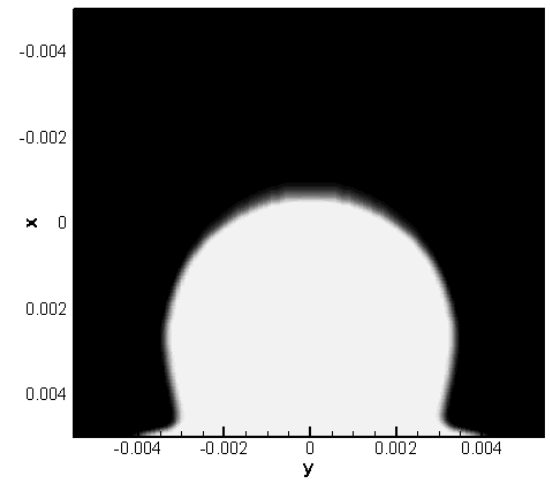
$t = 13.1\mu s$



Pressure



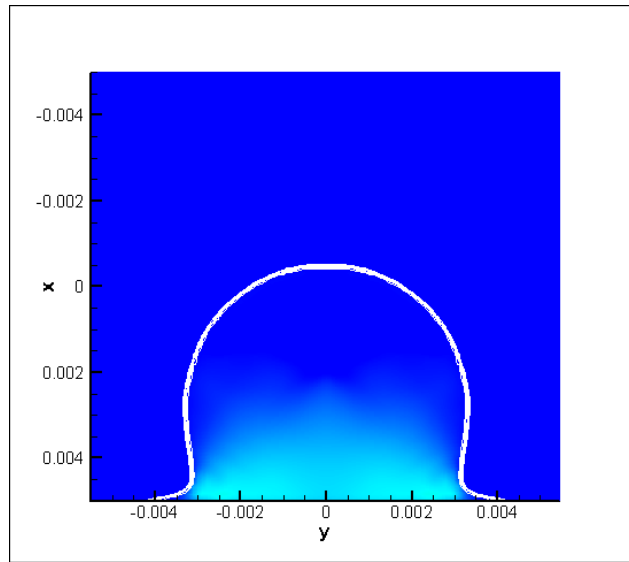
Velocity



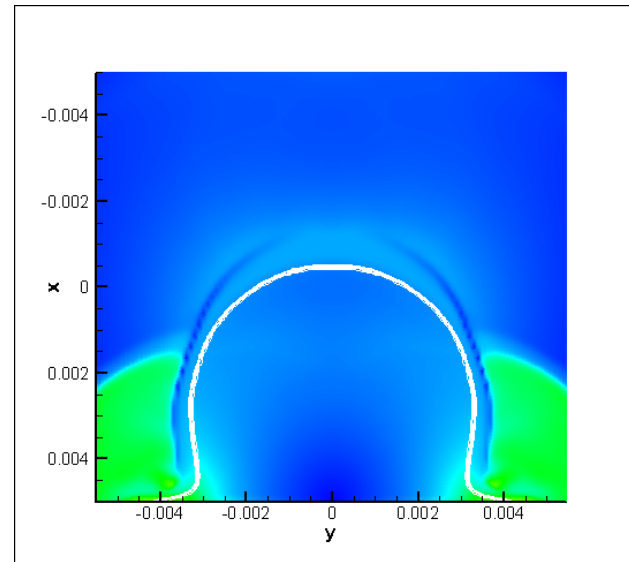
VOF



$t = 13.6\mu\text{s}$



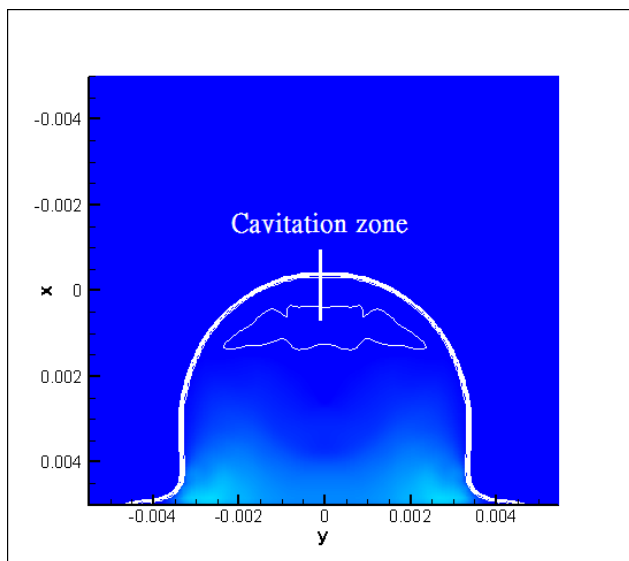
Pressure



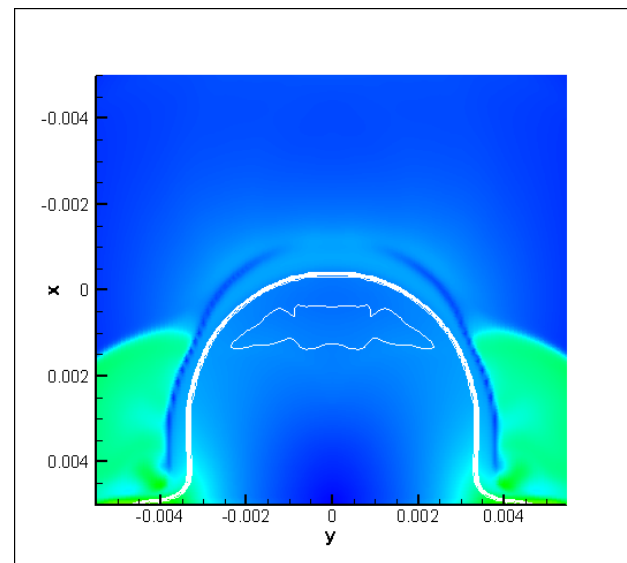
Velocity



$t = 14.4\mu s$



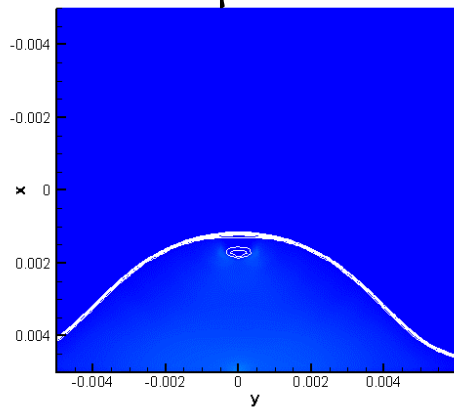
Pressure



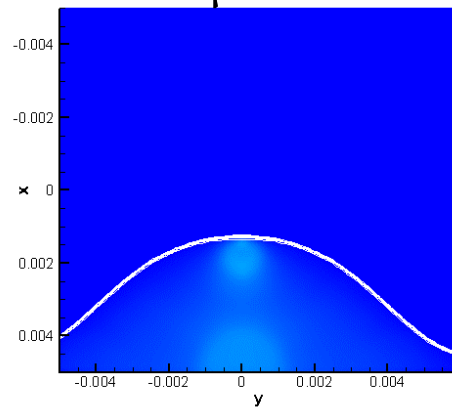
Velocity



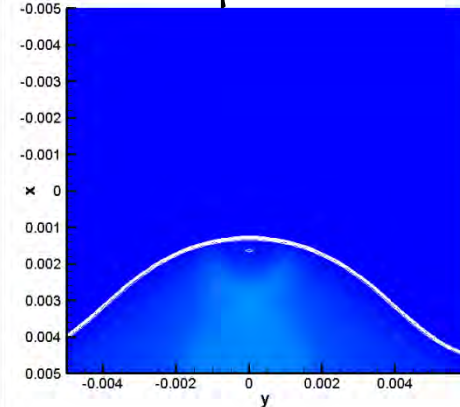
$t = 25.26\mu\text{s}$



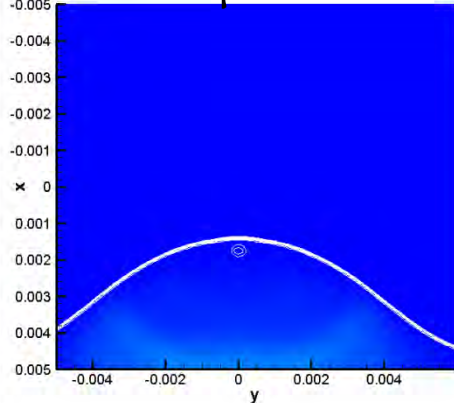
$t = 26.33\mu\text{s}$



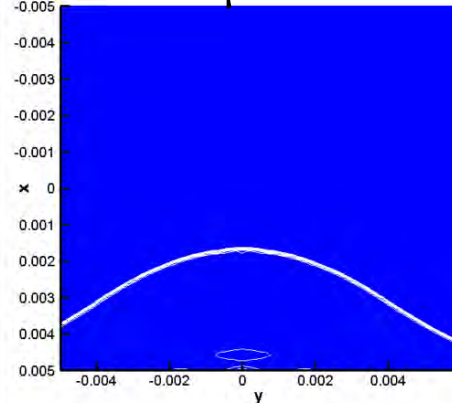
$t = 26.71\mu\text{s}$



$t = 27.82\mu\text{s}$

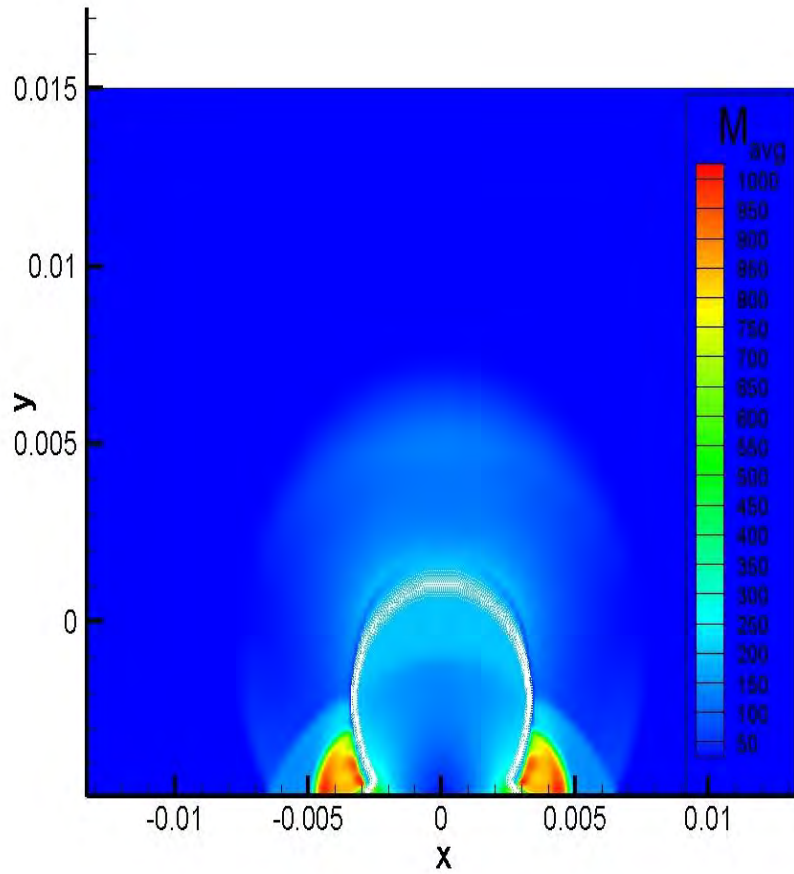


$t = 30.77\mu\text{s}$

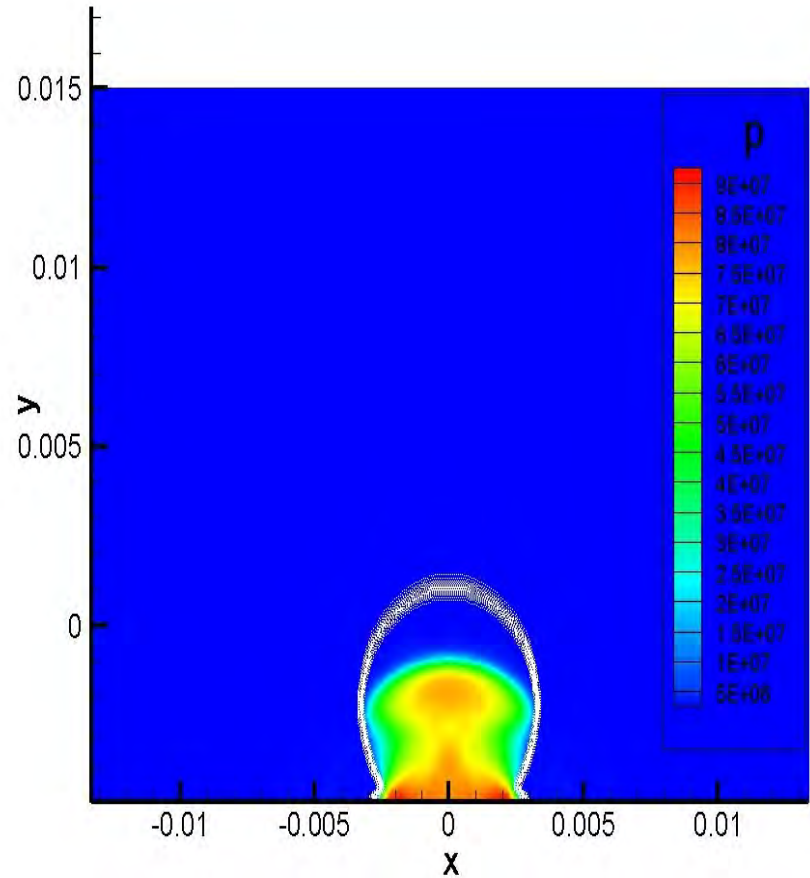




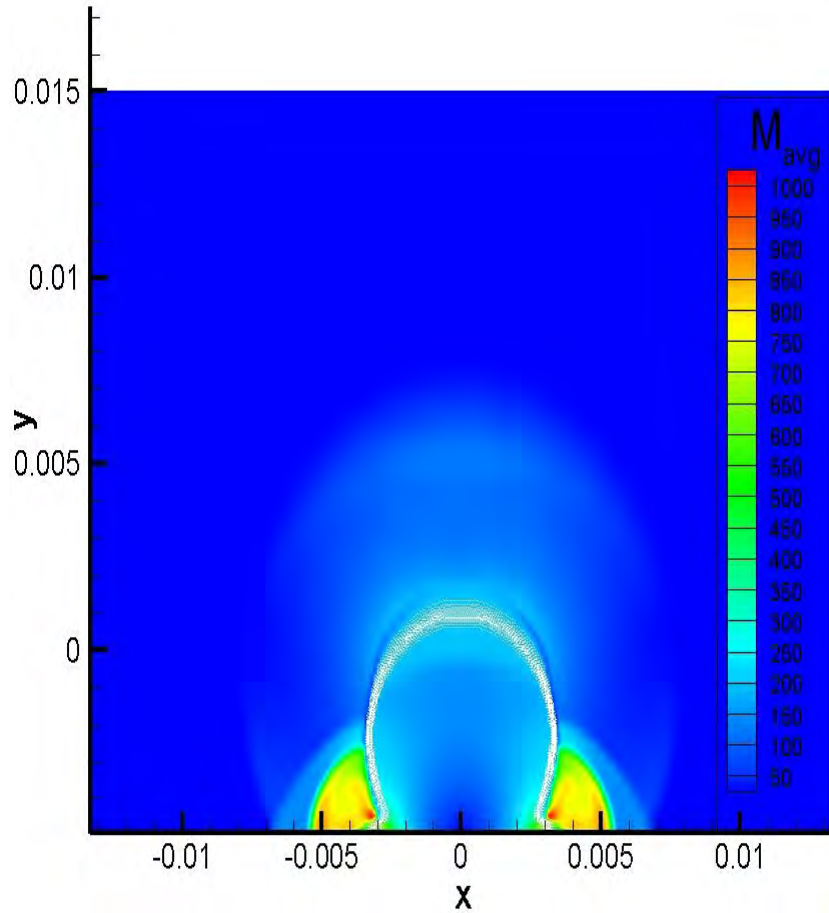
Wet Surface



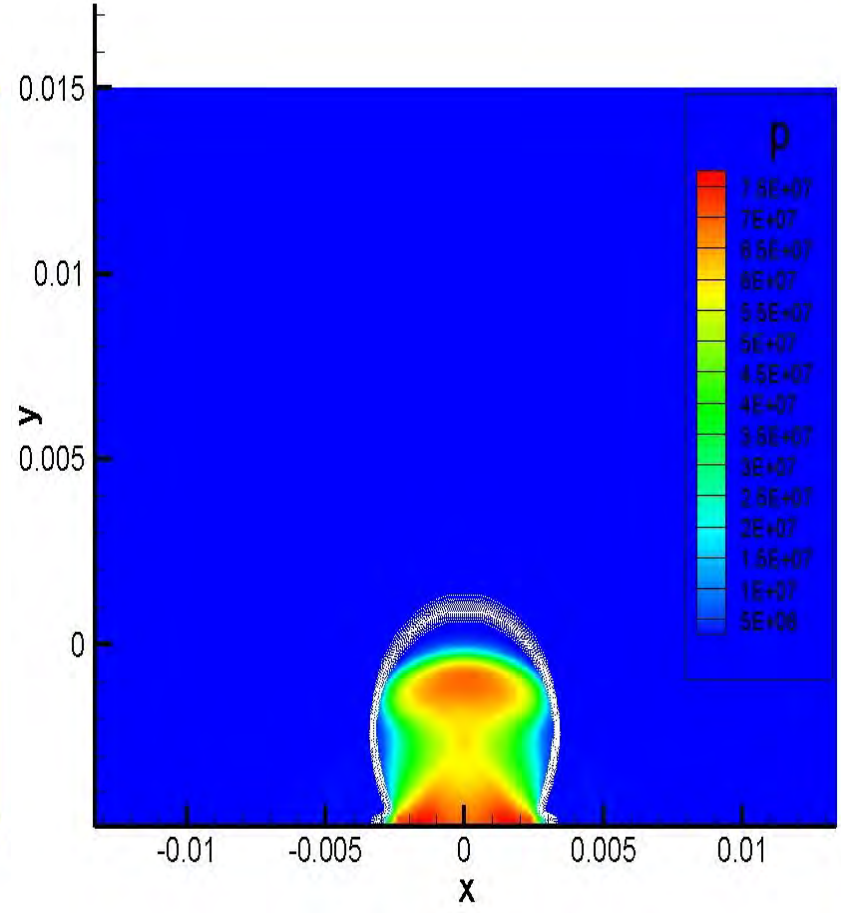
M_{avg}



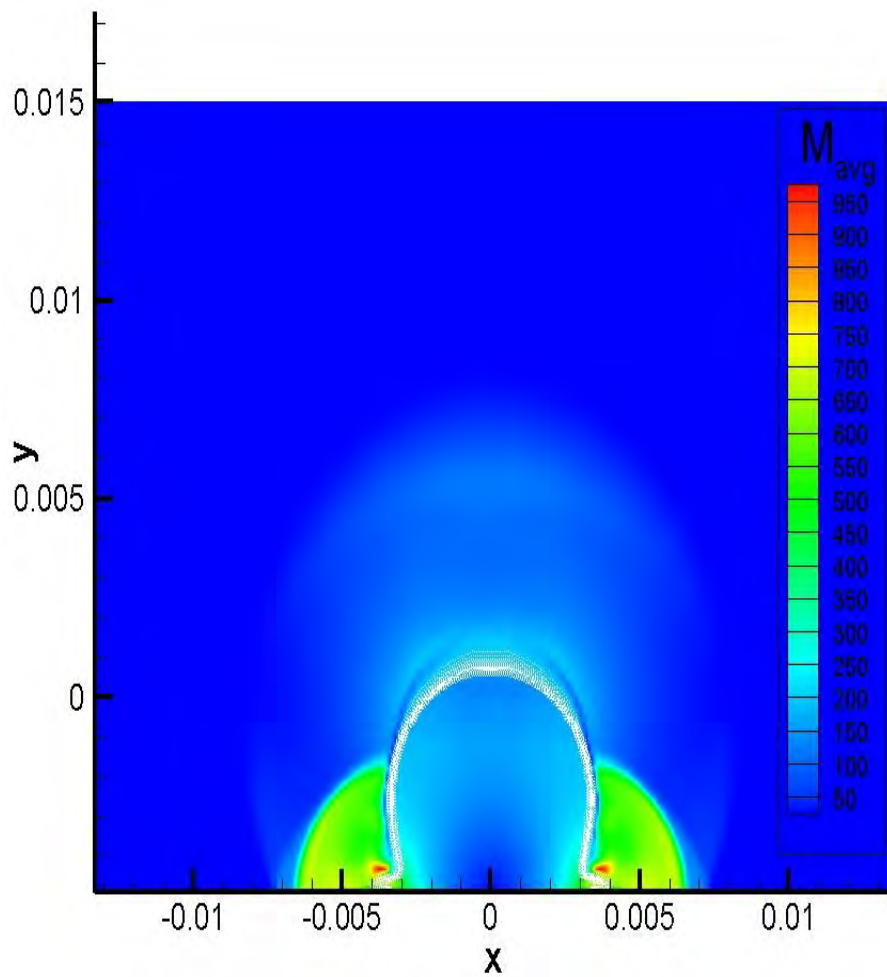
Pressure



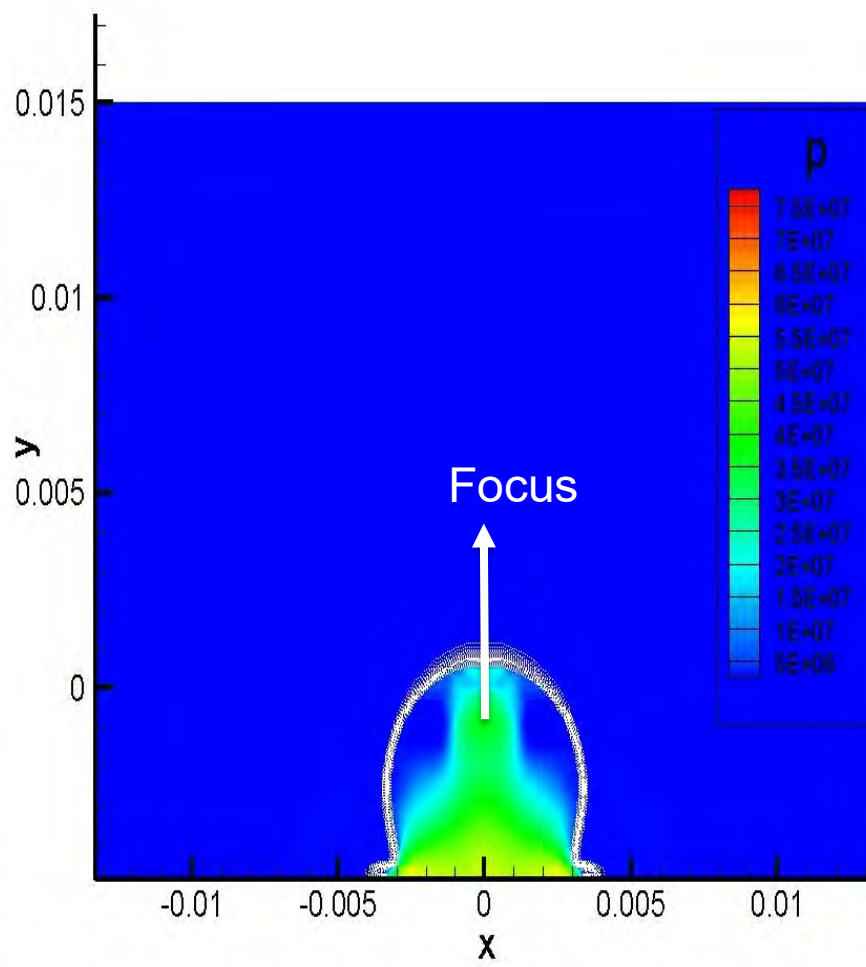
M_{avg}



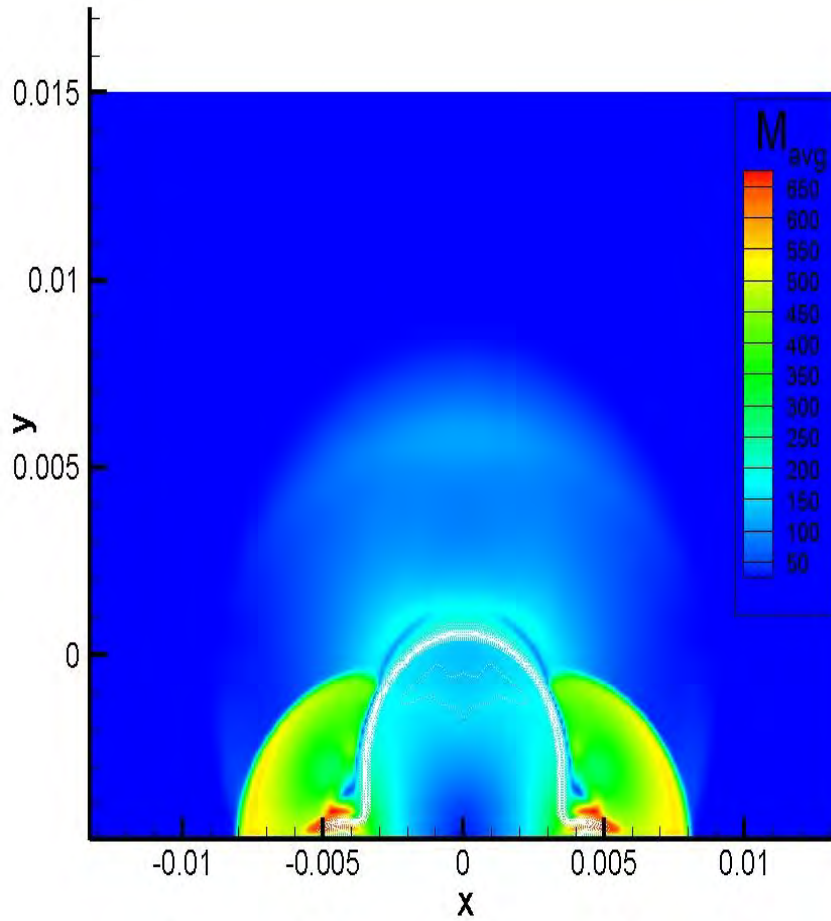
Pressure



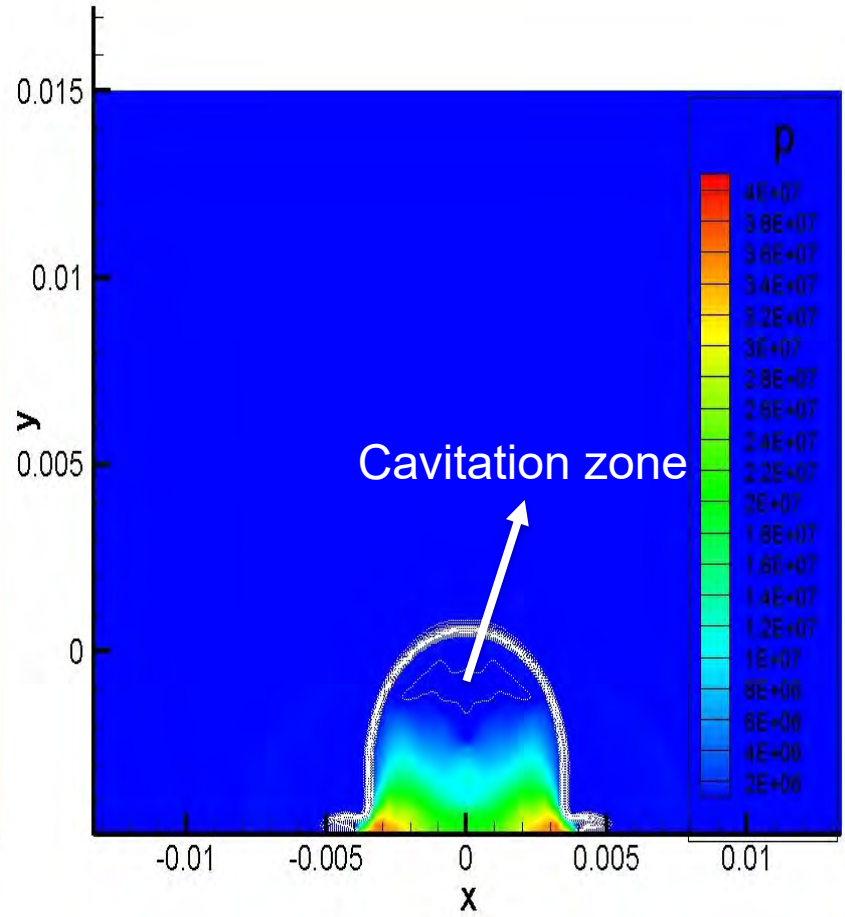
M_{avg}



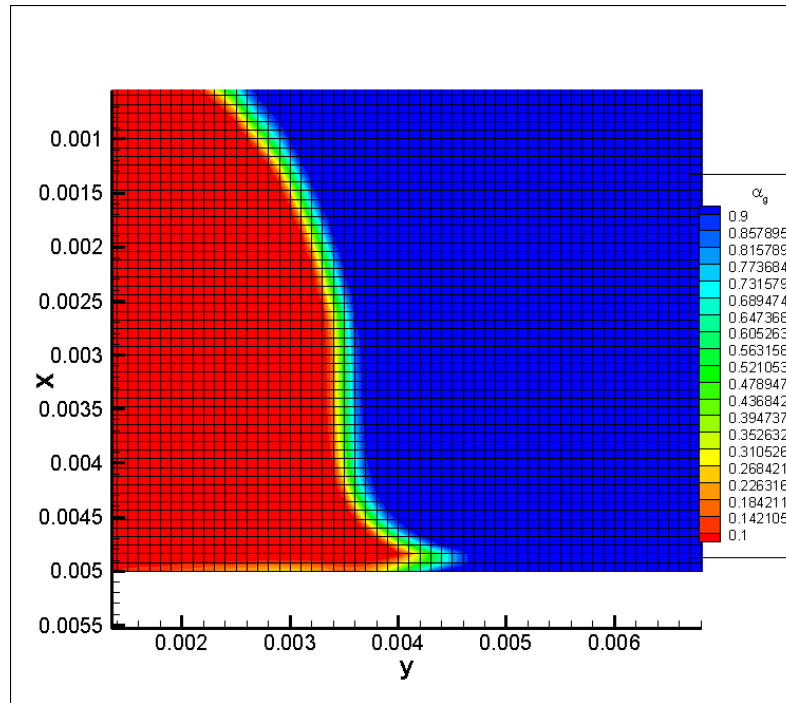
Pressure



M_{avg}



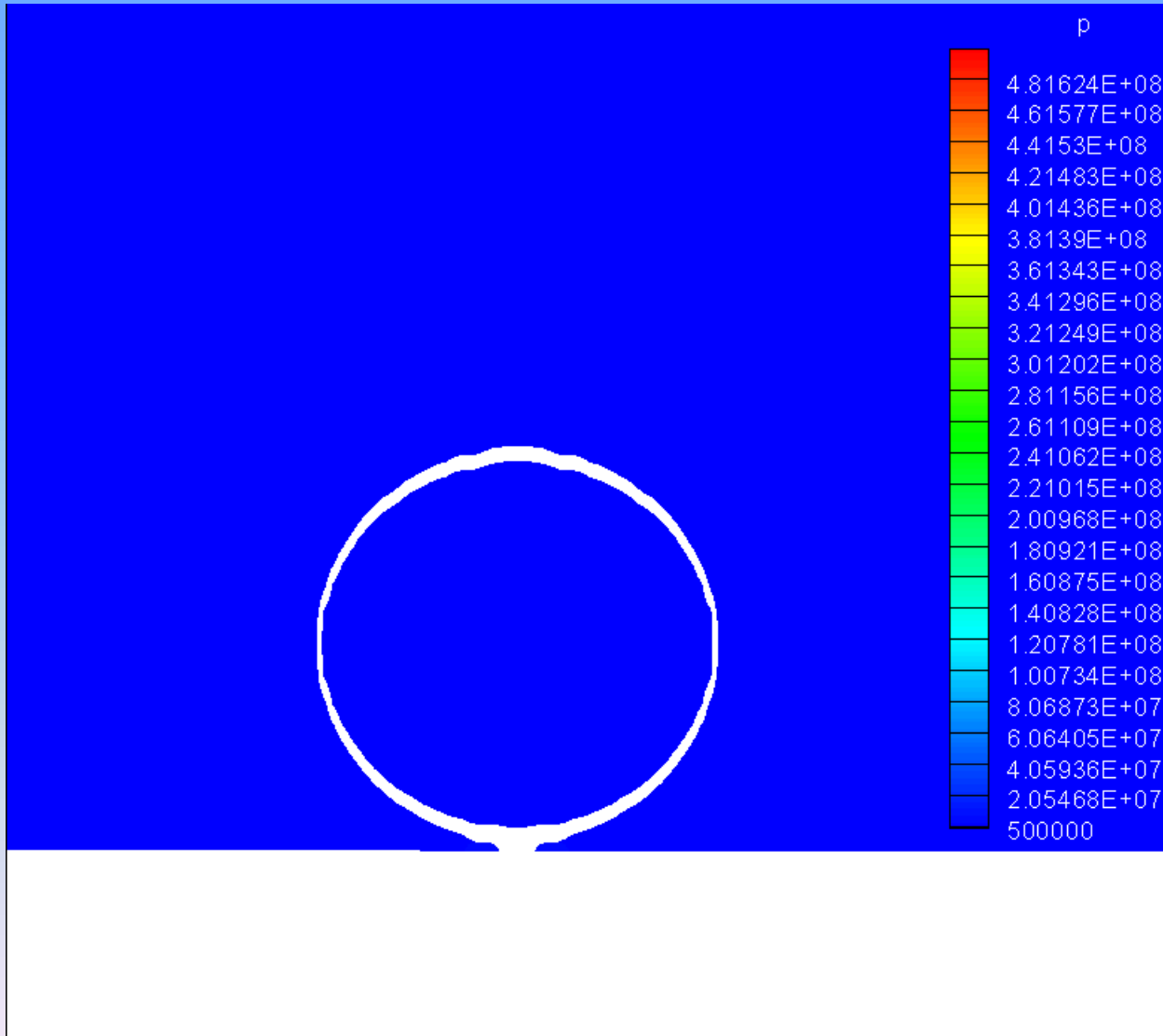
Pressure



(a) interface capturing on uniform grid



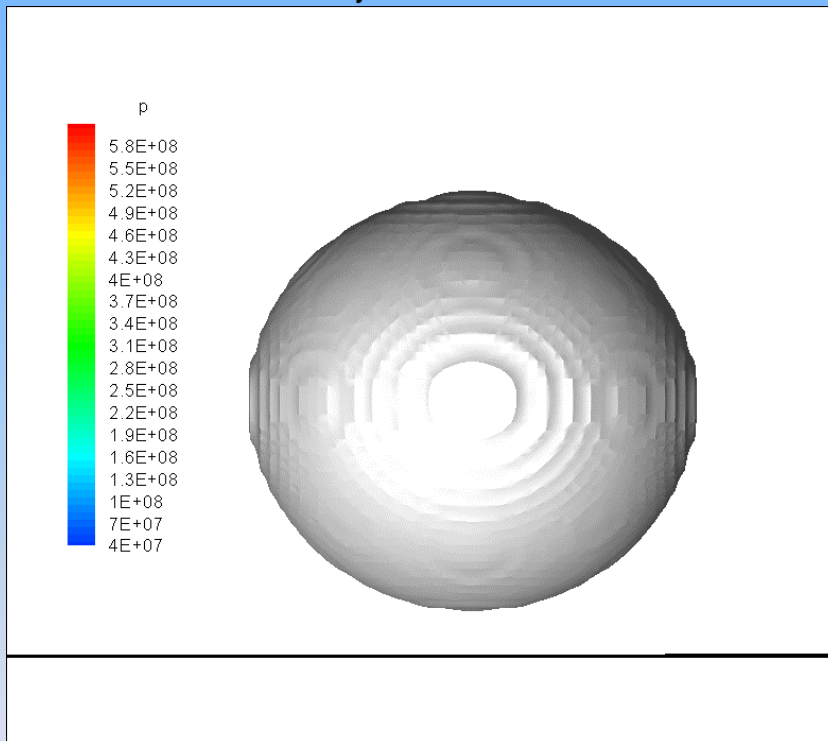
3D high-speed water droplet impact wall, $V=500\text{m/s}$



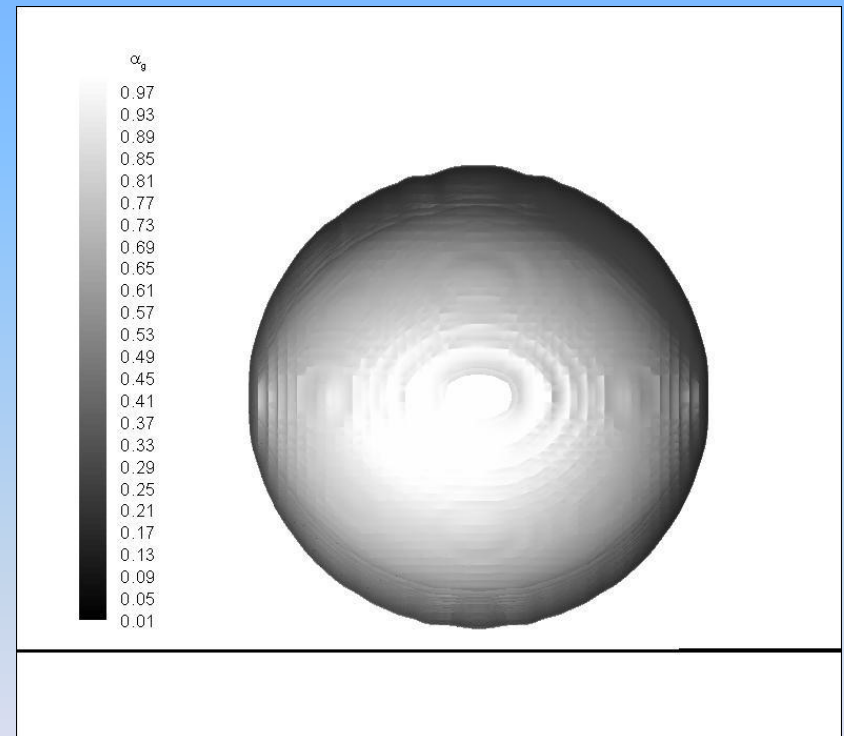


3D high-speed water droplet impact wall ($V=500\text{m/s}$)

$t = 3.0 \mu\text{s}$



Pressure

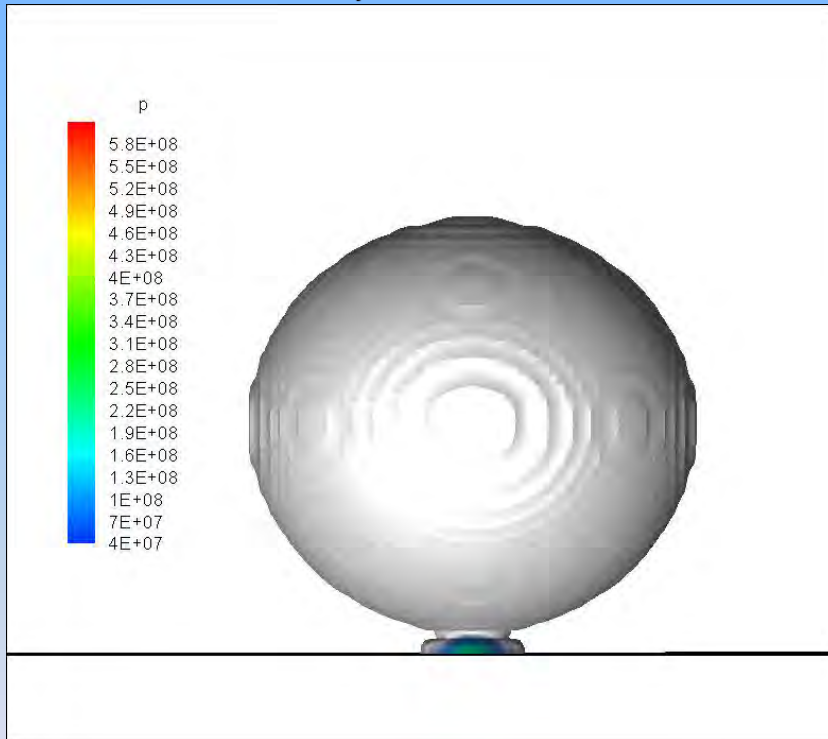


Volume of fraction

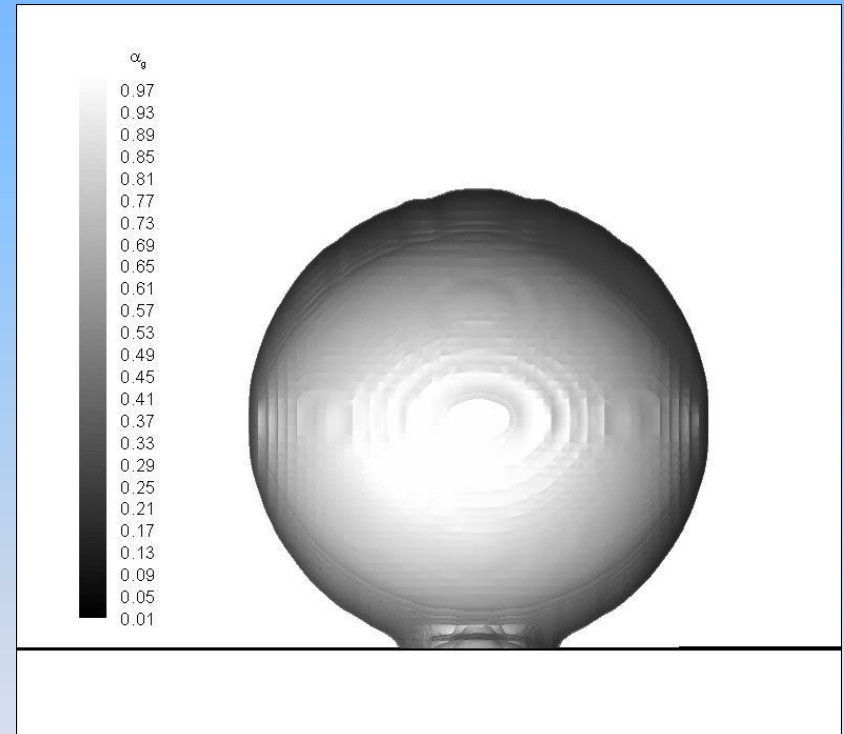


Case(VII):3D high-speed water droplet impact wall ($V=500\text{m/s}$, 0°)

$t = 3.7 \mu\text{s}$



Pressure

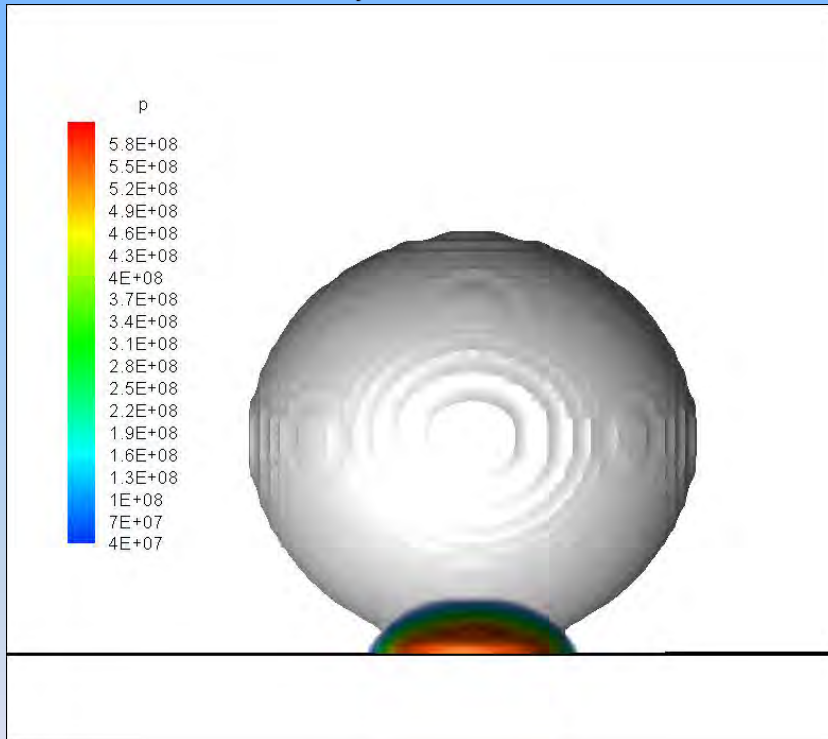


Volume of fraction

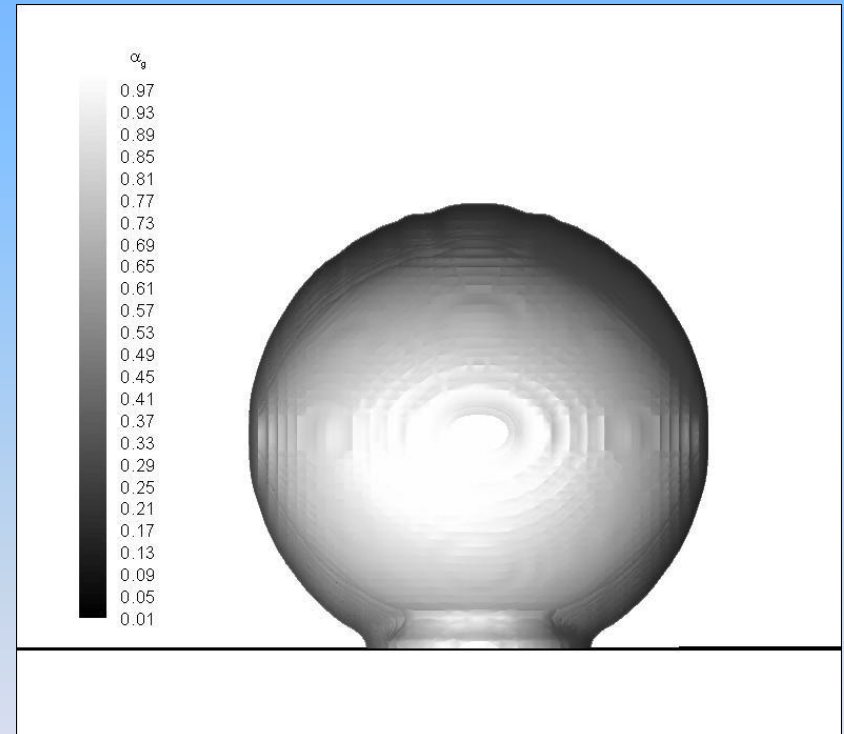


Case(VII):3D high-speed water droplet impact wall ($V=500\text{m/s}$, 0°)

$t = 4.1 \mu\text{s}$



Pressure

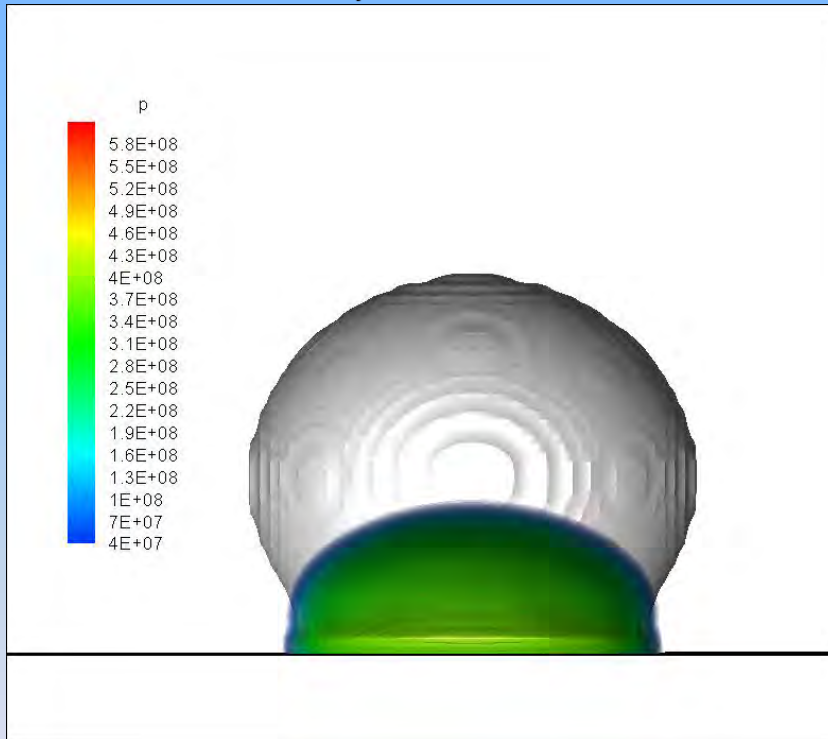


Volume of fraction

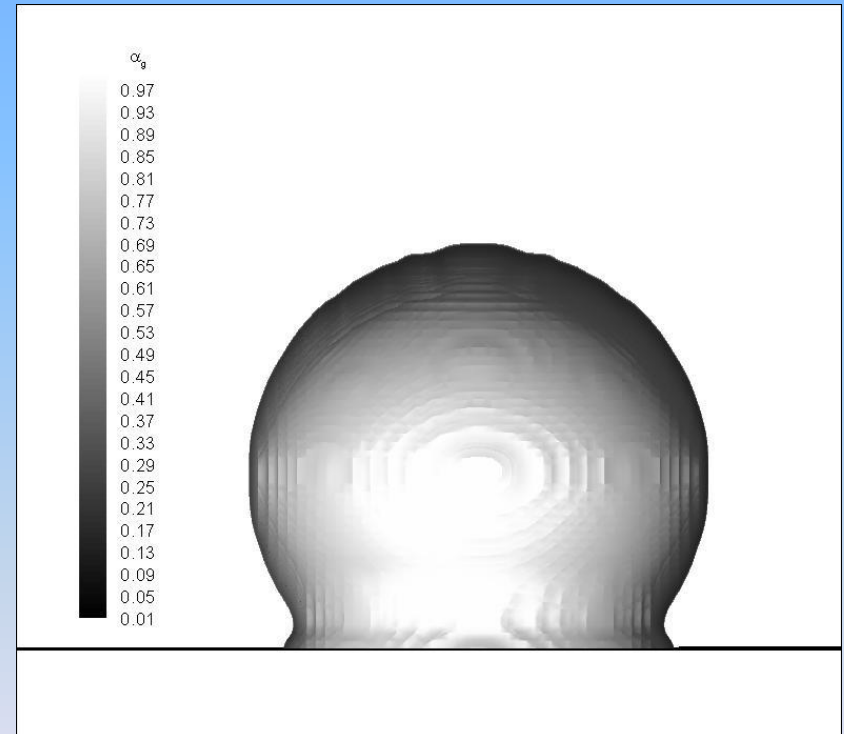


Case(VII):3D high-speed water droplet impact wall ($V=500\text{m/s}$, 0°)

$t = 5.2 \mu\text{s}$



Pressure

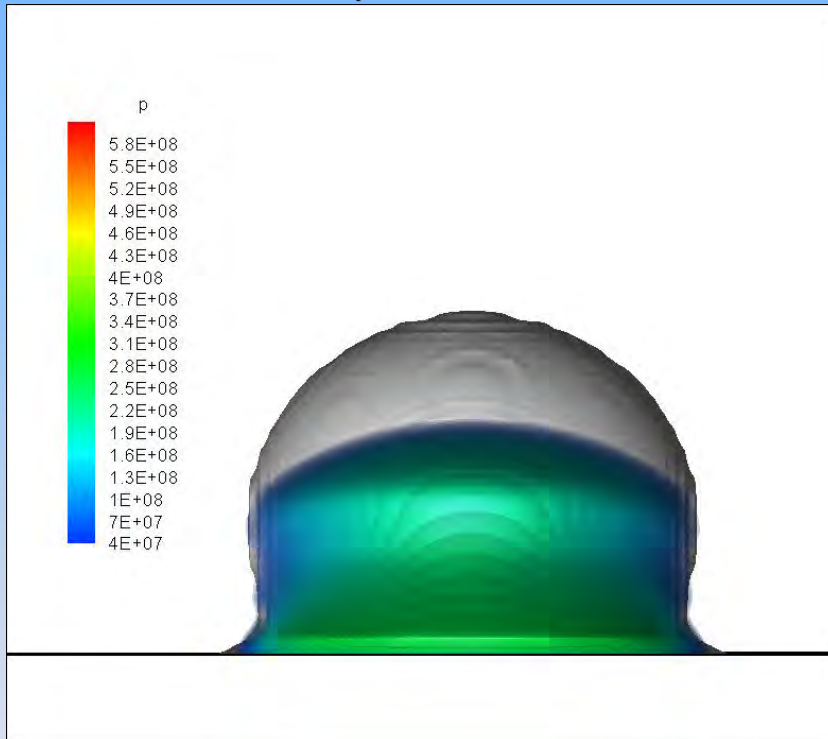


Volume of fraction

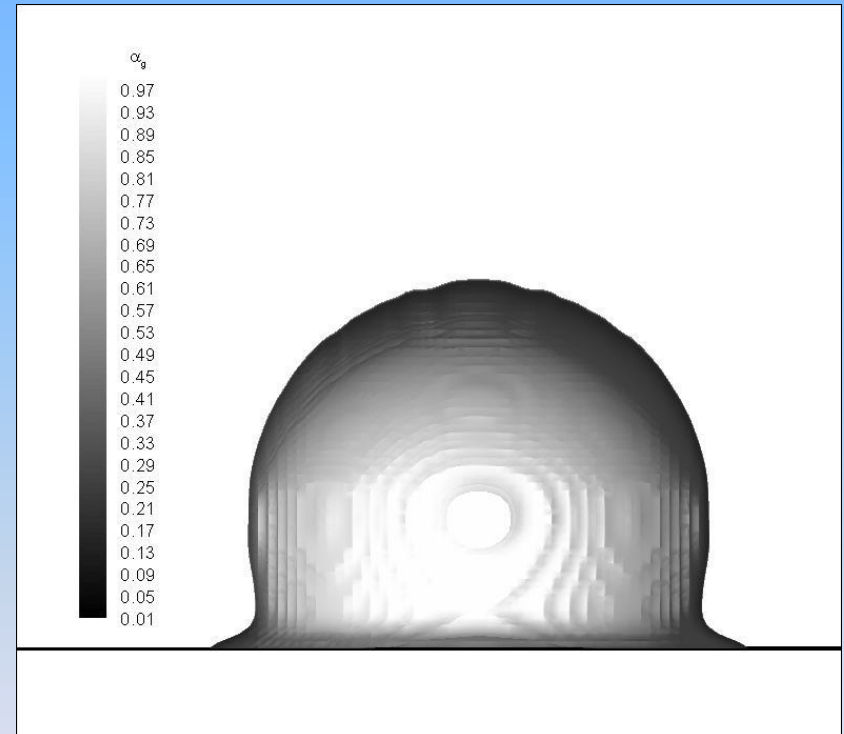


Case(VII):3D high-speed water droplet impact wall ($V=500\text{m/s}$, 0°)

$t = 6.2 \mu\text{s}$



Pressure

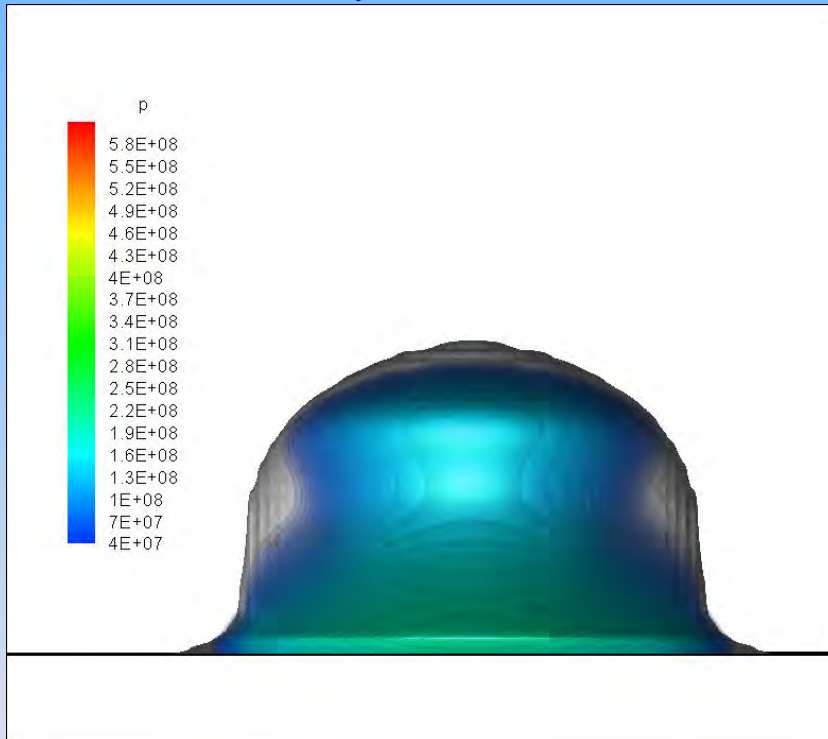


Volume of fraction

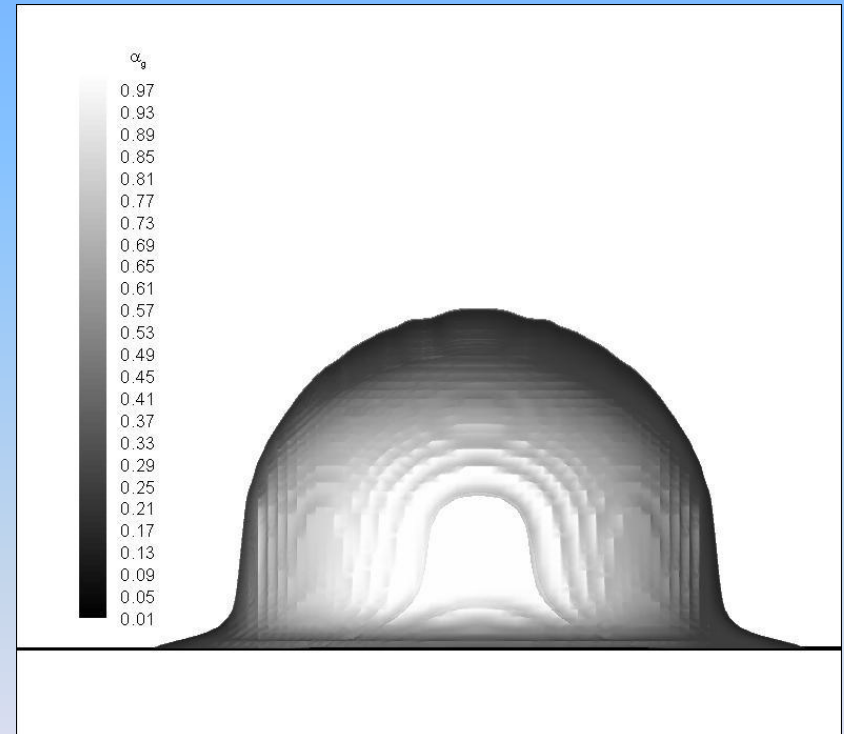


Case(VII):3D high-speed water droplet impact wall ($V=500\text{m/s}$, 0°)

$t = 7.0 \mu\text{s}$



Pressure

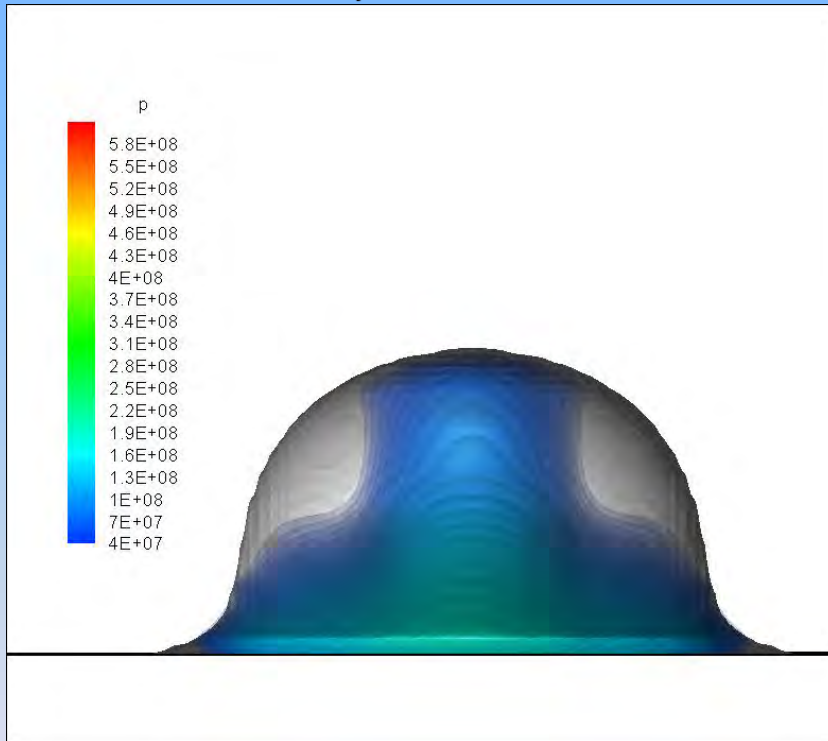


Volume of fraction

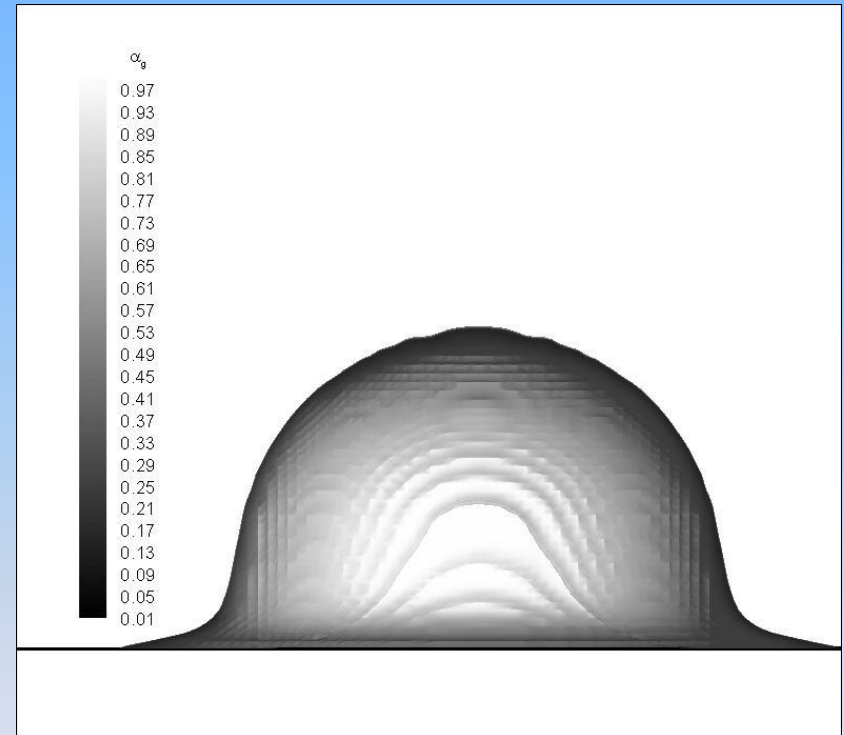


Case(VII):3D high-speed water droplet impact wall ($V=500\text{m/s}$, 0°)

$t = 7.5 \mu\text{s}$



Pressure

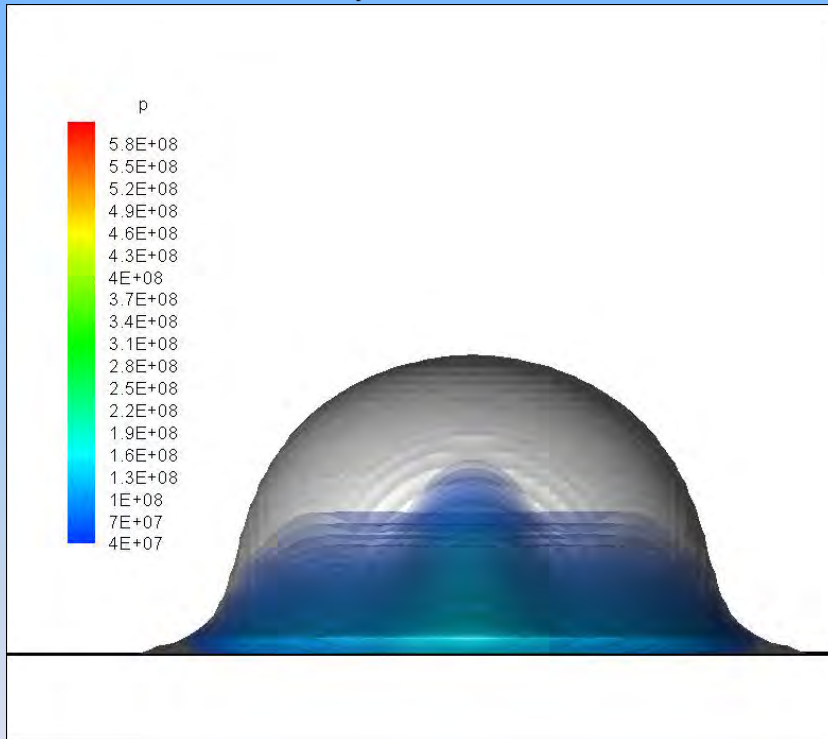


Volume of fraction

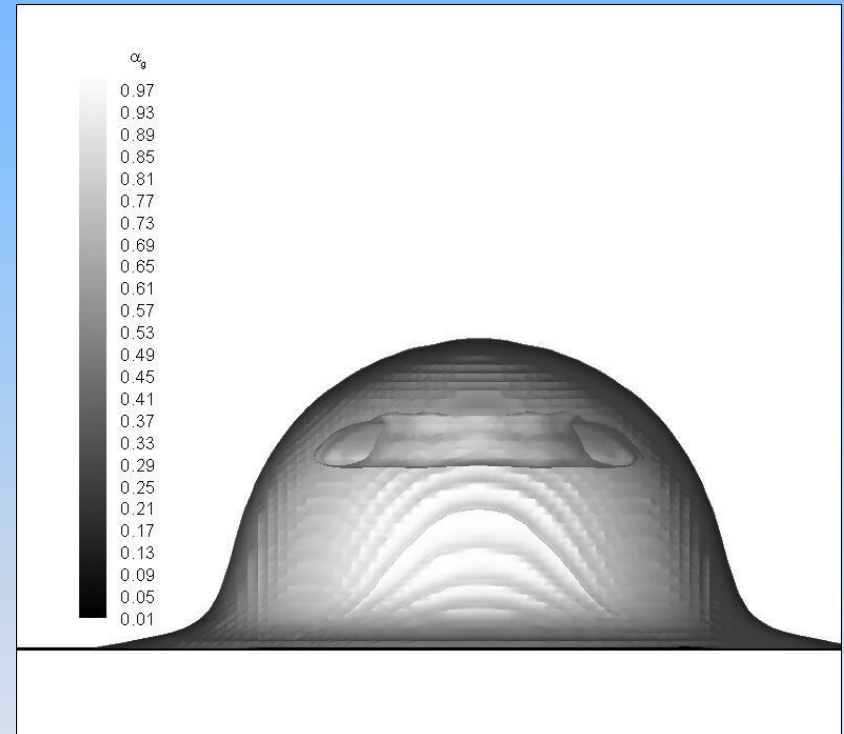


Case(VII):3D high-speed water droplet impact wall ($V=500\text{m/s}$, 0°)

$t = 7.9 \mu\text{s}$



Pressure

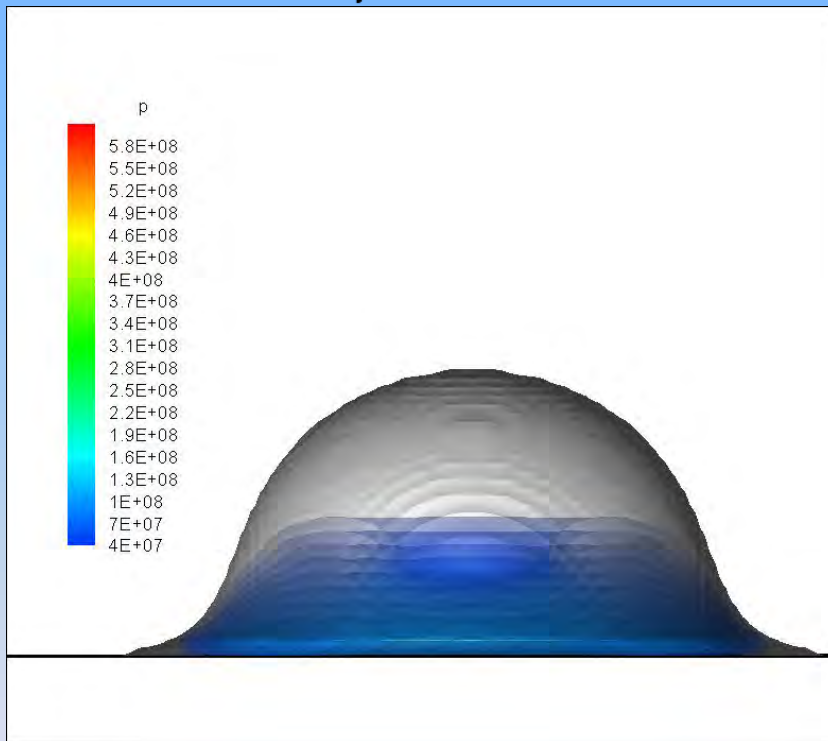


Volume of fraction

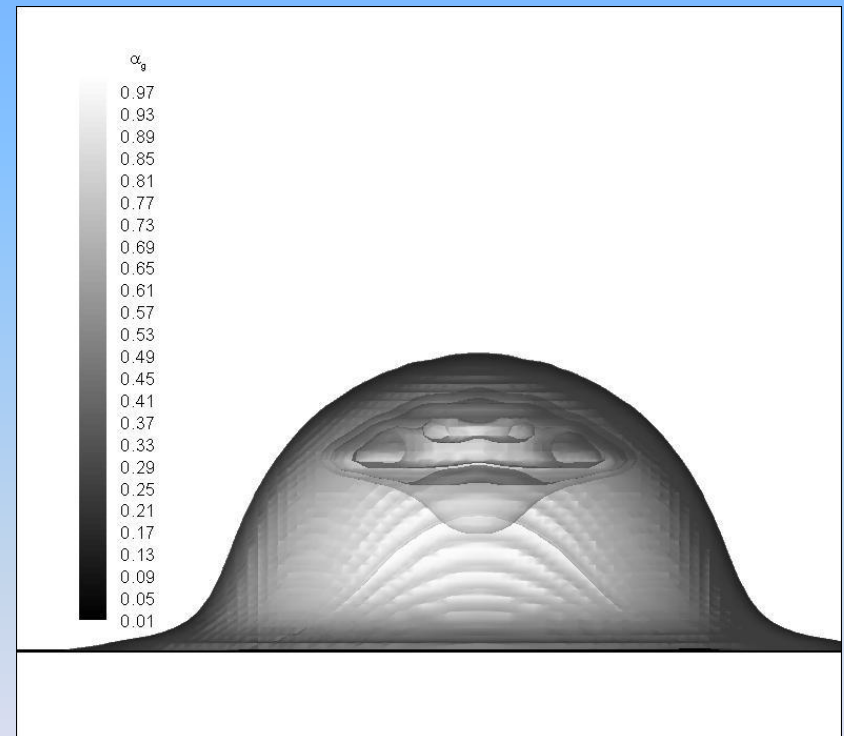


Case(VII):3D high-speed water droplet impact wall ($V=500\text{m/s}$, 0°)

$t = 8.4 \mu\text{s}$



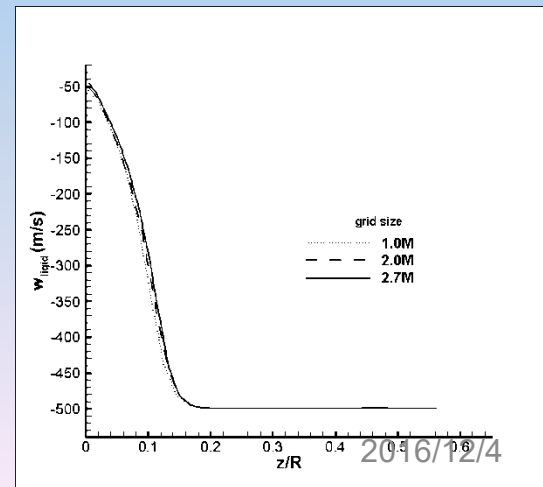
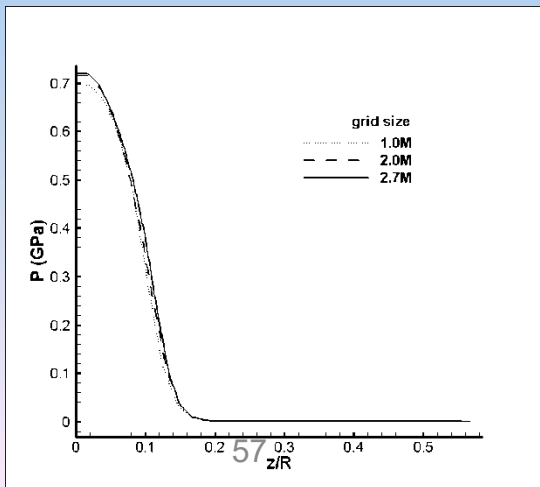
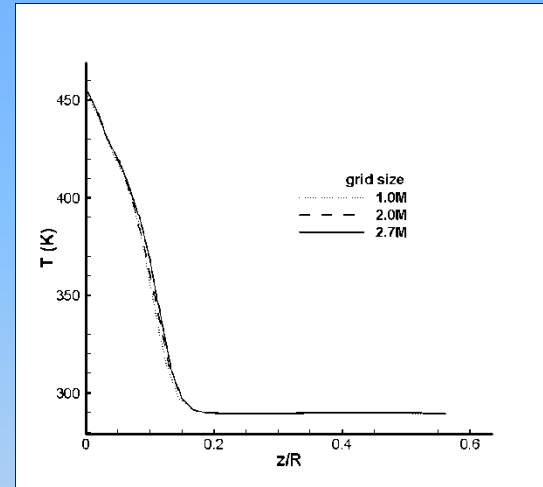
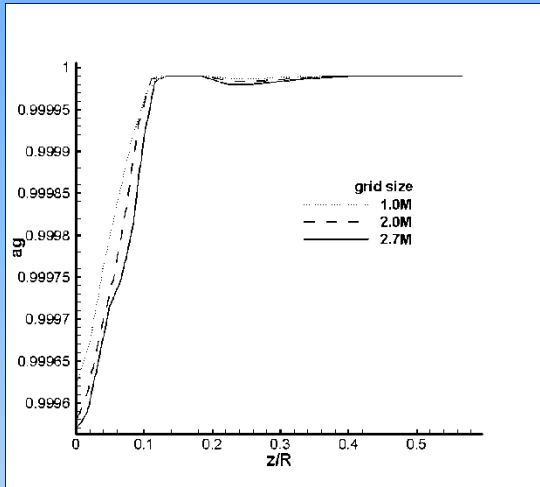
Pressure



Volume of fraction



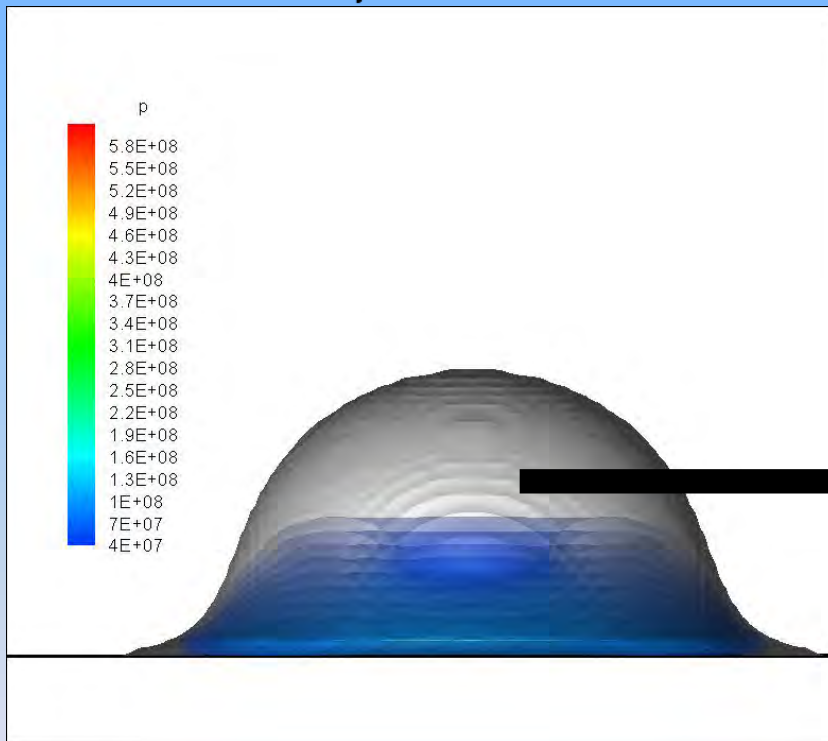
Grid Independence of 3D $V=500\text{m/s}$



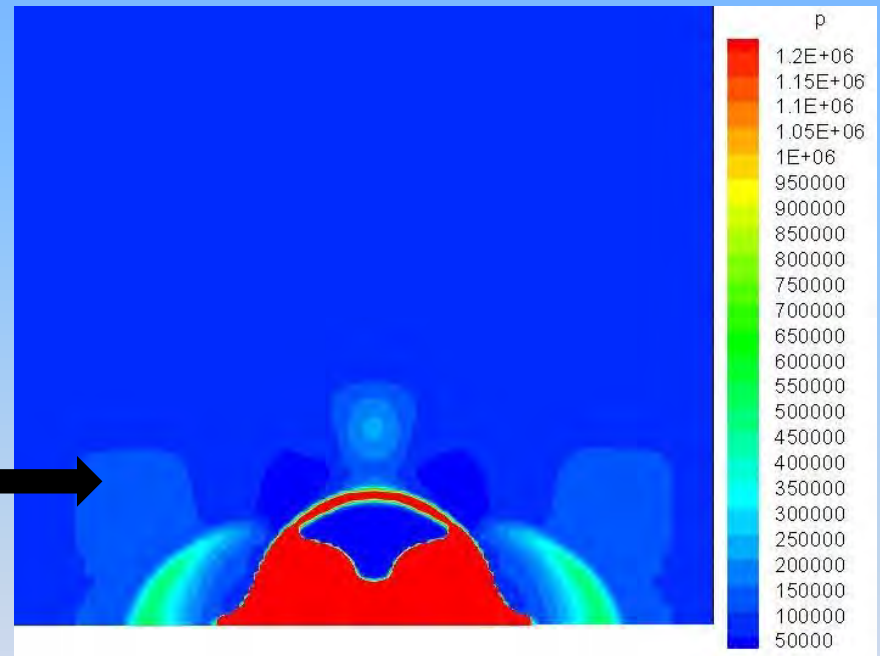


Case(VII):3D high-speed water droplet impact wall ($V=500\text{m/s}$, 0°)

$$t = 8.4 \mu\text{s} \quad \alpha = 1\text{e-}6$$



Pressure

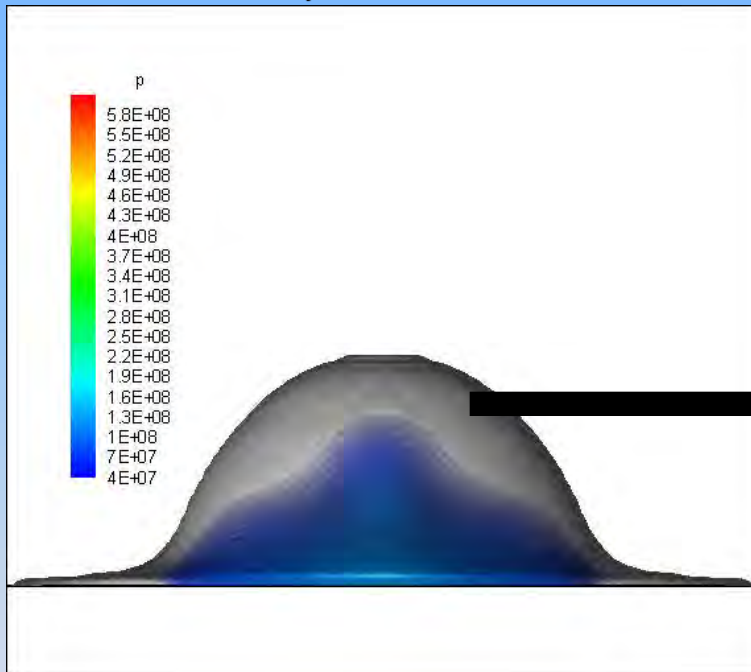


The lower pressure region sketch at the same time

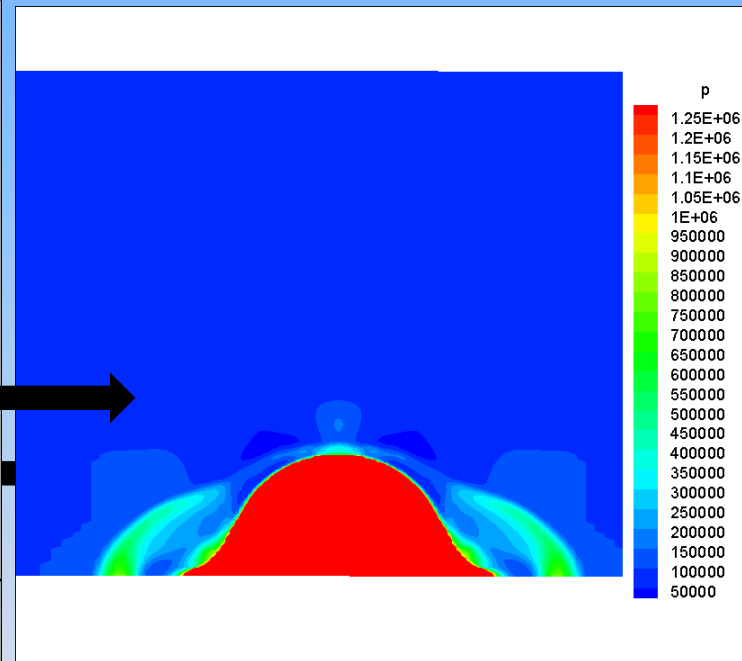


Case(VII):3D high-speed water droplet impact wall (V=500m/s,)

$t = 8.4 \mu s$ $\alpha = 0.018$



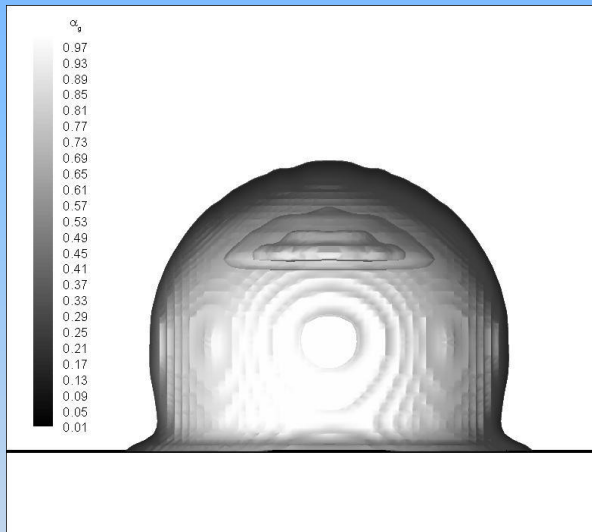
Pressure



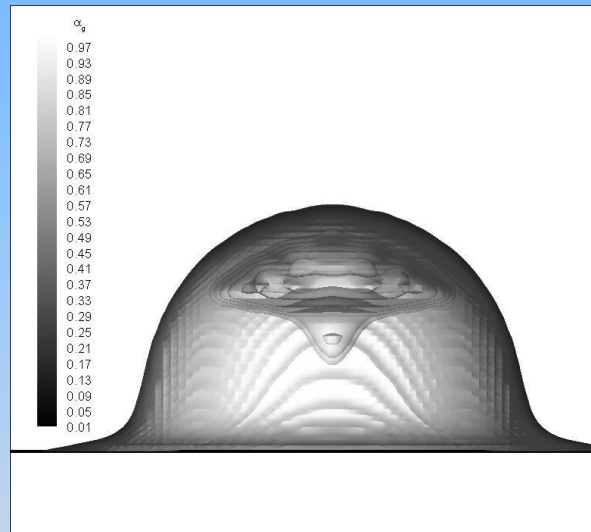
The lower pressure region sketch at the same time



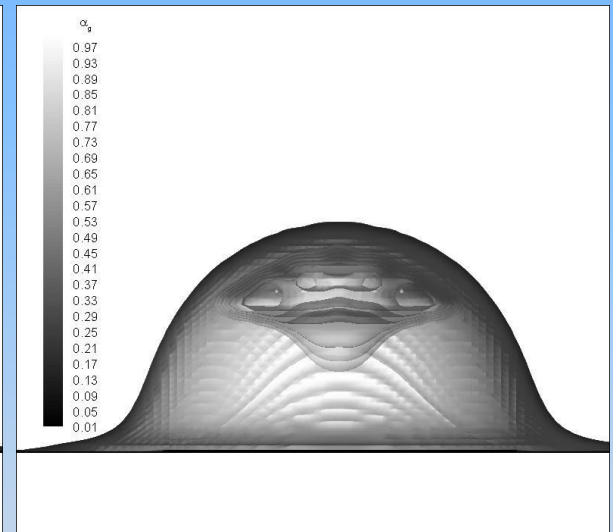
The cavitation area .vs. impact velocity



$V = 200 \text{ m/s}$
 $t = 15 \mu\text{s}$



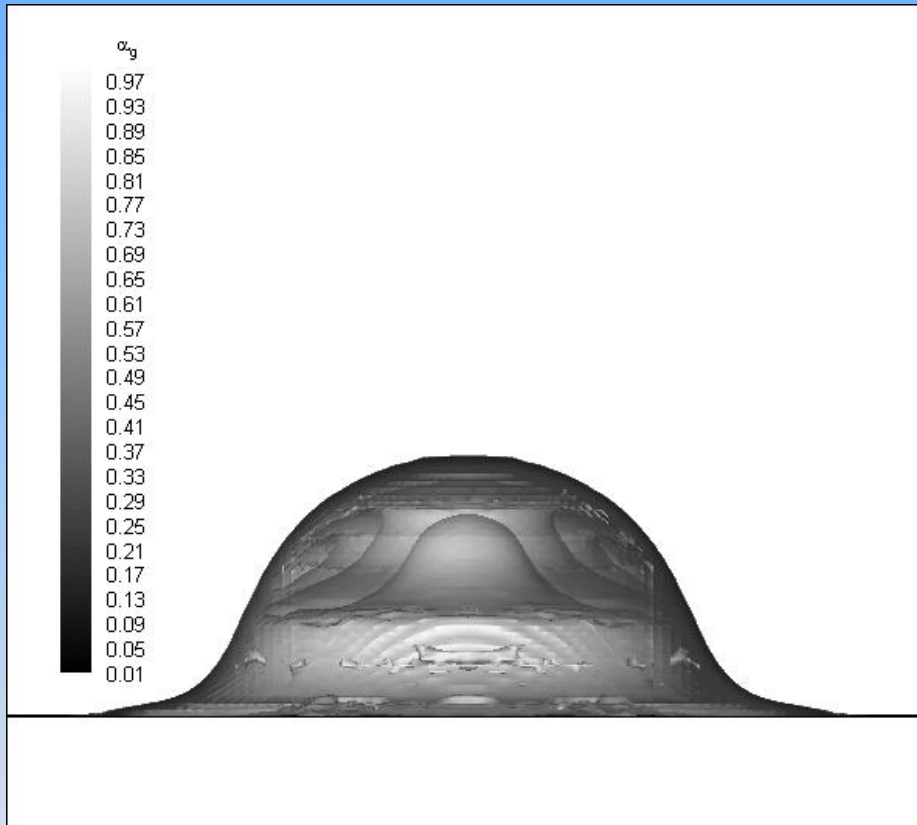
$V = 400 \text{ m/s}$
 $t = 9.6 \mu\text{s}$



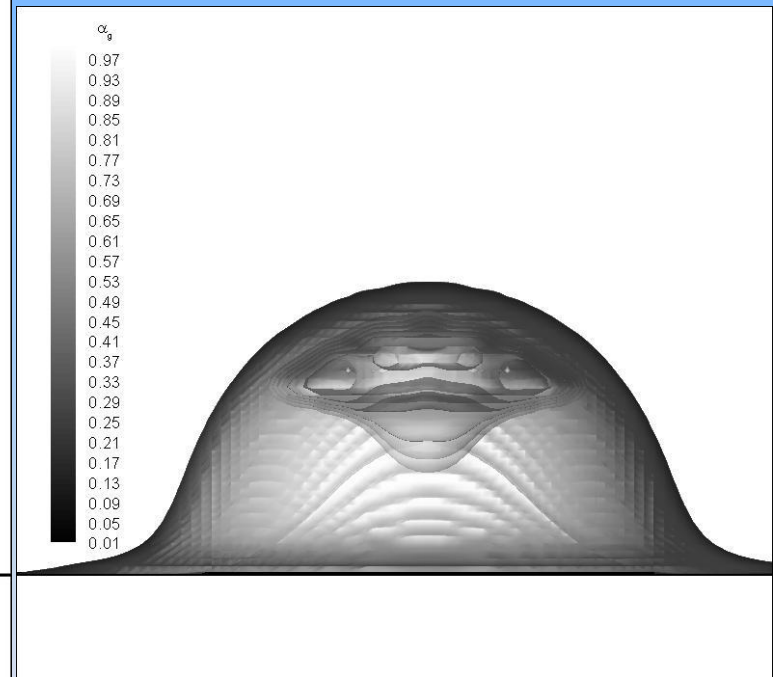
$V = 500 \text{ m/s}$
 $t = 8.4 \mu\text{s}$



The cavitation area .vs. initial conditions



$\alpha=0.018$



$\alpha=1e-6$



- 3D droplet impact animation



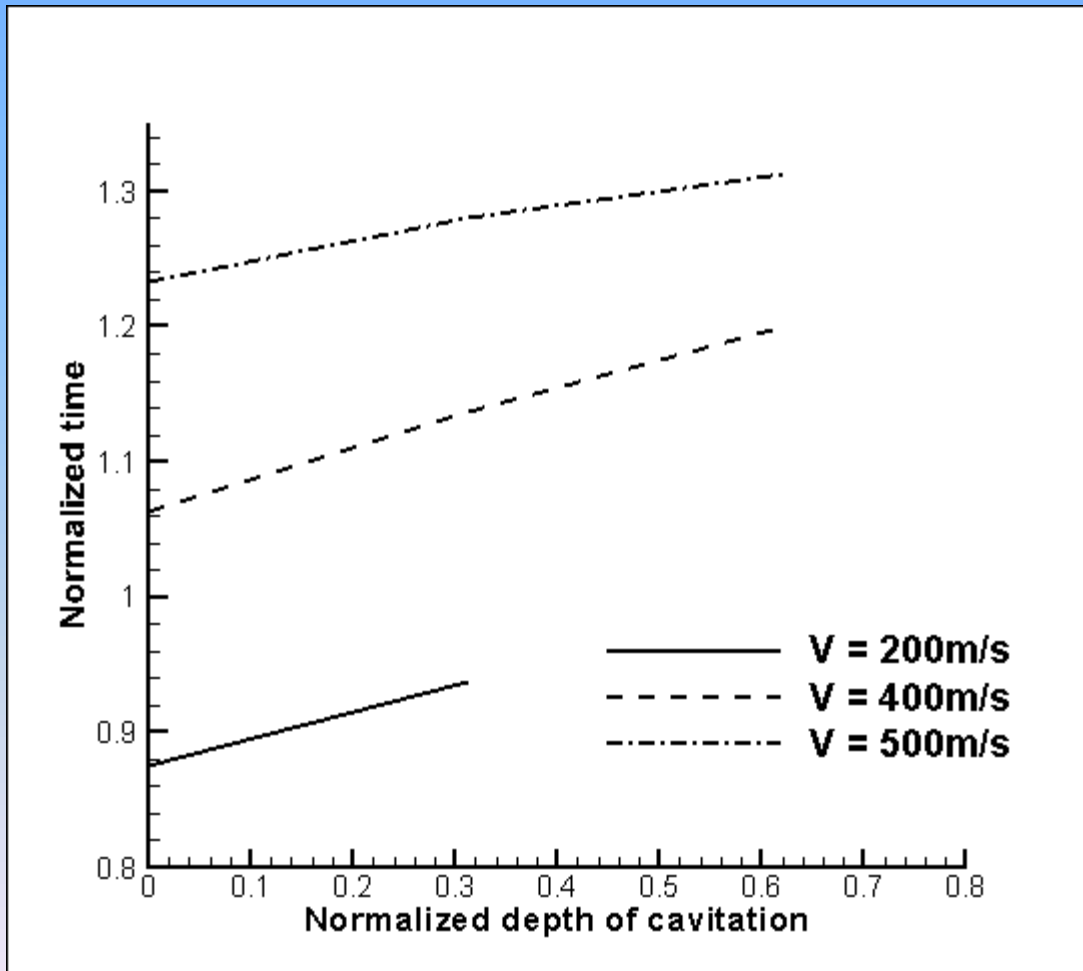
淡江大學航空太空工程學系

THE END

Thanks For Your Listening



The Growth Rate of Cavitation .vs. Time





Normalized pressure versus Impact Mach No.

